To be published in: *Molecular Electronics*, ed. by J. Jortner and M. A. Ratner (Blackwell, Oxford)

Coulomb Blockade and Digital Single-Electron Devices

Alexander N. Korotkov

Department of Physics, State University of New York, Stony Brook, NY 11794-3800 and

Nuclear Physics Institute, Moscow State University, Moscow 119899, Russia

Abstract

Tunneling of single electrons has been thoroughly studied both theoretically and experimentally during last ten years. By the present time the basic physics is well understood, and creation of useful single-electron devices becomes the important issue. Single-electron tunneling seems to be the most promising candidate to be used in the future integrated digital circuits with the typical size scale of few nanometers and below, i.e. in the molecular electronics. In the review we first briefly discuss the physics of single-electron tunneling and the operation of the single-electron transistor. After that, we concentrate on the hypothetical ultradense digital single-electron circuits and discuss the different proposed families of them. The last part of the review considers the issues of the discrete energy spectrum and the finite tunnel barrier height which are important for the molecular-size single-electron devices.

I. INTRODUCTION

The continuous trend in scaling down the component size leads the integrated electronics into the domain of so-called "mesoscopics", the dimension area between the microscopic and macroscopic worlds. The Coulomb blockade and other single-electron charging effects (for other reviews see, e.g., Refs. [1–5]) are among the most prominent phenomena of mesoscopic physics. Despite these effects are caused by single electrons that makes a connection with microscopic world, they are usually well-described in terms of macroscopic "electrical-engineering" quantities like capacitances and resistances. Single-electron effects will play an important role in almost any electronic device with dimensions below ~ 30 nm. Moreover, they can be used as the new physical basis for the operation of nanoscale digital circuits.

The main component of single-electronics is a tunnel junction with a very small capacitance. These junctions can be implemented using a variety of materials: metal-insulator-metal structures, GaAs quantum dots, silicon structures, large molecules with conducting cores, etc. If the size (and, hence, the effective electrical capacitance C) of the junction is sufficiently small, then the tunneling of only one electron may produce a noticeable change e/C of the voltage across the junction. The discreteness of this change which is a consequence of the electrical charge discreteness, leads to a number of effects which constitute the field of single-electronics. The most widely known effect is the Coulomb blockade. This is the suppression of tunneling at voltages |V| < e/2C because in this case the tunneling would increase the electrostatic energy of the capacitor: $C(V \pm e/C)^2/2 > CV^2/2$. Besides the "Coulomb blockade" and "single-electronics", the other key words of the field are "correlated tunneling" and "single charge tunneling".

The typical capacitance in most present day experiments is on the order of 10^{-16} F (the simplest well-established technology uses metal junctions with an area about 50×50 nm²). It corresponds to the voltage scale e/C on the order of one millivolt that is already sufficiently large to allow experimental studies. To avoid the smearing of single-electron effects by thermal fluctuations, the thermal energy k_BT should be much less then the typical

one-electron charging energy,

$$k_B T \ll e^2 / 2C. \tag{1}$$

For $C \approx 10^{-16}$ F this condition limits the temperature to $T \lesssim 1$ K. As a consequence, at the present stage of development, the practical use of single-electron devices is limited to scientific experimentation and fundamental metrology. To achieve the real industrial impact, the operation temperature must be increased up to 300 K (or at least to 77 K) that requires a dramatic decrease of the typical size of the components. There is already a considerable number of experiments in which the room temperature or liquid nitrogen temperature operation of simple single-electron "devices" was reported, but these systems are not well-controllable and reproducible so far.

Capacitances as small as 10^{-19} F can be achieved in principle in the "molecular electronic devices" using conducting clusters of atoms (with diameter of 1 nm or even less) embedded in a molecular matrix. In this case the energy scale $e^2/2C$ would be about one electron-volt, and the room temperature operation could be ensured. Notice that at the size scale below few nanometers, single-electronics gradually enters the areas of chemistry and atomic physics. Here, the discreteness of energy levels in conducting "islands" becomes an important factor, the electric capacitance becomes a not well-defined quantity, and the Coulomb blockade energy gradually converts into the energy of ionization and electron affinity. However, the ideas of single-electronics are applicable even at this size scale, opening the possibility of information processing in molecular-based devices.

II. BRIEF HISTORY

The influence of the single-electron effects on the conductance of thin granular metallic film was understood at least by Gorter [6] as early as in 1951. During the next 20 years important contributions to this field came from the papers by Neugebauer and Webb [7], Giaver and Zeller [8], and Lambe and Jaklevic [9]. The first quantitative theory for a two-junction system was developed in 1975 by Kulik and Shekhter [10].

In the present-day meaning the single-electronics was launched in the mid-1980s when the detailed theory of correlated tunneling (now known as the "orthodox" theory) developed by Averin and Likharev [11,12] was almost immediately supported by first experiments with single-electron transistors [13,14]. Since that time there was a constantly growing interest both in theoretical and experimental single-electronics, so that the total number of publications by the present time is well above a thousand.

Single-electron effects were studied experimentally using various materials and technologies. The oldest and most developed technique is the fabrication of small tunnel junctions by overlapping narrow strips of metal films using electron beam patterning and double-angle evaporation (see, e.g., Refs. [13,15–26]). Among the best achievements towards possible applications, let us mention single-electron transistors with the charge sensitivity better than $10^{-4}e/\sqrt{\text{Hz}}$ (at 10 Hz) [27], low-temperature absolute thermometer with $\sim 1\%$ accuracy [28], the prototype of the dc current standard with the relative accuracy better than 10^{-6} [29], and the single-electron trap ("memory cell") with the retention time more than 12 hours [30].

Since 1990 [31] single-electron charging effects are also studied in tunneling through small islands ("quantum dots") of 2D electron gas in GaAs-based heterostructures. It was predicted [32] that in these structures the coexistence of the energy and charge quantizations should play a much more important role than in metal islands of comparable size. This fact was soon confirmed experimentally [33,34] (now the structures exhibiting both types of quantization are sometimes called "artificial atoms" [5]). The study of single-electron

effects in the systems of quantum dots was so far of mainly scientific interest (see, e.g., the latest papers [35–39]), and their technology is still too far from possible applications. As an exception let us mention the experiment [40] in which the side-gated constrictions in δ -doped GaAs were used to demonstrate the operation of the few-electron "memory cell" at 4 K. The Coulomb barrier in this case appears due to tunneling between randomly positioned small conducting islands in the constriction.

There is a considerable number of experiments in which single electrons tunnel from the tip of scanning tunneling microscope to the substrate via a small conducting particle (see, e.g. Refs. [41–51]). The effect may survive up to the room temperature for sufficiently small metal particles [45,46], and it can be even stronger when the tunneling via single molecules is studied [47–51]. Scanning tunneling microscope can be also used for the fabrication of the single-electron circuits [52].

Quite promising results were obtained recently in the experiments with silicon-based structures [53–57]. The memory effects and the operation of single-electron transistor were reported even at room temperature. Taking into account the huge experience accumulated in silicon technologies, the silicon-based devices could be a real way to the integrated single-electronics.

Ultradense integrated circuits is the most intriguing goal of the single-electronics. There were many theoretical suggestions on this topic. Let us mention the digital circuits based on single-electron transistors [12,58–60], the logic which uses single electrons to represent logic bits [61–66] (including various "wireless" logics [67,68]) and background-charge-independent devices [69]. The practical realization of the integrated single-electron circuits remains quite a questionable issue because very serious technological problems should be solved to reach this goal. Nevertheless, the rapid progress in experimental single-electronics during a few last years combined with the rapid improvement of the nanotechnology makes room temperature single-electronics a candidate for the next generation of ultradense digital devices.

III. "ORTHODOX" THEORY OF SINGLE-ELECTRONICS

The main object of the single-electronics is a small tunnel junction. The simplest approach described below works very well for metallic junctions. Several specific features of semiconductor and molecular-level systems will be considered in Section VI.

The tunnel junction consists of two electrodes separated by an insulating layer and naturally has some electric capacitance C depending on the geometry (in the simple case of the plain capacitor $C = \varepsilon \varepsilon_0 S/d$ where S is the area, d is the insulator thickness, and ε is its dielectric constant). In contrast to the usual capacitor, in the tunnel junction electrons can pass through a sufficiently thin barrier (typically several nanometers). Let us assume the linear I - V curve (in the absence of single-electron effects), I = V/R, that is the typical case for metallic systems.

The "orthodox" single-electronics [1] deals with junctions having sufficiently large resistances,

$$R >> R_O = \pi \hbar / 2e^2 \approx 6.4k\Omega.$$
 (2)

To understand the physical meaning of this condition let us notice that the rate of tunneling in a junction biased by some voltage V is $\Gamma = V/eR$ so that the typical time between tunneling events is $1/\Gamma = eR/V$. The "duration" of a tunneling event due to the uncertainty principle is \hbar/eV (there are several other definitions of the tunneling time – see, e.g. Ref. [70], however, they are not relevant to this problem). Hence, Eq. (2) simply means that the tunneling events do not overlap, and we can speak about the separate tunneling of single electrons.

In the case of small capacitance C the voltage $V = V_b$ before the tunneling event is considerably different from the voltage $V_a = V_b - e/C$ after the event. Hence, it is not clear which value should be used for the calculation of the tunneling rate. The simple guess is that we can take the average value as the effective voltage

$$V_{eff} = \frac{V_b + V_a}{2} = V_b - \frac{e}{2C}. (3)$$

This guess coincides with the result of the "orthodox" theory. In fact, the effective voltage should be related to the change W of the electrostatic energy of the system (energy gain due to tunneling). In the case of a single capacitor charged initially by Q = CV this change will be

$$W = \frac{Q^2}{2C} - \frac{(Q - e)^2}{2C} = e(V - \frac{e}{2C}) = eV_{eff}, \tag{4}$$

that coincides with Eq. (3). This derivation is still valid if we consider the tunnel junction being a part of the complex circuit. The only difference is that we need to use the effective (total) capacitance of the junction calculated with account of the rest of the circuit.

For a given energy gain W the tunneling rate in "orthodox" theory is calculated using the formula

$$\Gamma = \frac{W}{e^2 R (1 - \exp(-W/k_B T))} \tag{5}$$

where T is the temperature. In case of zero temperature this expression transforms to $\Gamma = V_{eff}/eR$ for positive $W = eV_{eff}$ and $\Gamma = 0$ for negative W.

Absence of tunneling for W < 0 is natural because the processes which increase the free energy are forbidden by the second principle of thermodynamics. Using Eq. (4) we see that W < 0 if the voltage across the junction is less than the threshold value $V_t = e/2C_{eff}$ that corresponds to the charge Q = e/2. This is the condition of the Coulomb blockade of tunneling (see Fig. 1). For finite temperature the tunneling inside the blockade region is possible but it is strongly suppressed as long as $k_B T << e^2/2C_{eff}$.

The electron transport in an arbitrary single-electron circuit consisting of tunnel junctions, capacitors, and voltage sources is described by the "orthodox" theory as a sequence of jumps of single electrons. For any given charge state of the system one should calculate the tunneling rates for all junctions. In which particular junction and at what exactly moment the next tunneling will occur, is a matter of chance with the probabilities determined by the corresponding rates. After the jump the charge state changes, and one should calculate all rates anew. These rates determine the probability distribution for the next jump, and so

on. This scheme may be used to implement a Monte-Carlo algorithm [71] for the simulation of the electron transport. Another approach [10,1] is to solve the kinetic equation

$$\frac{d}{dt}p(k) = \sum_{m \neq k} p(m) \Gamma(m \to k) - p(k) \sum_{m \neq k} \Gamma(k \to m) \quad \sum_{k} p(k) = 1,$$
 (6)

which describes the evolution of the probability distribution p(k) among all possible charge configurations.

The "orthodox" theory can also treat the systems with Ohmic resistances, if they are considerably larger than the quantum unit R_Q . According to the fluctuation-dissipation theorem the spectral density of the quantum fluctuations of current through the Ohmic resistance R_0 is $S_I(\omega) = 2\hbar\omega/R_0$ (at zero temperature). Corresponding r.m.s. fluctuations of the charge can be estimated as $\Delta q \sim (S_I(\omega)\Delta\omega)^{1/2}/\omega \sim (\hbar/R_0)^{1/2}$ for $\Delta\omega\sim\omega$. Hence, inequality $R_0 >> R_Q$ allows to neglect the quantum fluctuations of the charge, $\Delta q << e$. Such an Ohmic resistor is considered in "orthodox" theory as an open circuit when the effective capacitances are calculated. (One can say that the charge transferred through R_0 "during" the tunneling event is negligible, $(e/C)/R_0 \times \hbar/(e^2/C) << e$.) The charge transfer through the resistor during the time between tunneling events leads to the gradual change in time of the tunneling rates (this change is stochastic at finite temperature due to Nyquist noise).

Despite its simplicity, the "orthodox" theory of single-electronics is sufficient to describe most experimental results quantitatively. Among the most important developments beyond the "orthodox" theory let us mention the account of arbitrary electrodynamic environment [72,73] (in particular, arbitrary ohmic resistances), the theory of simultaneous tunneling (cotunneling) in several junctions [74,75], and the account of energy quantization [76,32,77].

IV. SINGLE-ELECTRON TRANSISTOR

The most thoroughly studied single-electron device is the so-called Single-Electron Transistor [11,12] (dubbed as SET-transistor or SET) which is the simplest circuit in terms of fabrication. Its basic part consists of two tunnel junctions in series (Fig. 2a). Using this example, let us illustrate the use of the "orthodox" theory.

The voltage drops $V_{1,2}(n)$ across the junctions are functions of the number n of excess electrons on the central island

$$V_{j}(n) = V \frac{C_{1}C_{2}}{C_{i}C_{\Sigma}} + (-1)^{j} \frac{Q_{0} - ne}{C_{\Sigma}},$$
(7)

where V is the bias voltage, $C_{\Sigma} = C_1 + C_2$ is the total capacitance of the central island, and Q_0 is its initial (background) charge. The energy gain $W_j^{\pm}(n)$ due to tunneling (\pm denotes two different directions of tunneling) can be calculated as

$$W_i^{\pm}(n) = e(\pm V_j(n) - e/2C_{\Sigma}) \tag{8}$$

because the effective capacitance is C_{Σ} for any tunneling. The next step is the calculation of the rates $\Gamma_j^{\pm}(n)$ using Eq. (5). The stationary solution of the kinetic equation (6) for the probabilities p(n) of different charge states n is as follows

$$p_{st}(n) \times \left(\Gamma_1^+(n) + \Gamma_2^-(n)\right) = p_{st}(n+1) \times \left(\Gamma_1^-(n+1) + \Gamma_2^+(n+1)\right), \quad \sum p_{st}(n) = 1, \quad (9)$$

and the average (dc) current I can be calculated as

$$I = \sum_{n} p_{st}(n) (\Gamma_1^+(n) - \Gamma_1^-(n)). \tag{10}$$

Figure 3 shows several dc I-V curves of the symmetric double-junction system $(C_1 = C_2, R_1 = R_2)$ calculated in this way. The Coulomb blockade suppresses the current when the voltage is not sufficient to provide the energy for single-electron charging of the central island (notice also the rounding of the curve cusps due to finite temperature). The threshold voltage V_t depends on the background charge, and its maximal value is e/C_{Σ} . The same value determines the I-V curve offset at large voltages, $I=(V-e/C_{\Sigma})/R_{\Sigma}$. The Coulomb

blockade completely disappears $(V_t = 0)$ for half-integer background charge, $Q_0 = (k+1/2)e$, because the states with effective charges e/2 and -e/2 have equal energies. The current is a periodic function of Q_0 (Fig. 4) because the addition of the integer electron charge is compensated by the tunneling of one electron in or out of the central island. This periodic dependence is usually called Coulomb oscillations. Very high (subelectron) sensitivity to the charge of the central island is the basis of the SET-transistor operation. Controlling Q_0 by capacitively coupled gate (C-SET, Fig. 2b) or via coupling resistor (R-SET, Fig. 2c), one controls the flow of electrons tunneling through the SET-transistor.

R-SET is quite difficult to implement because the coupling resistance R_g should be much larger than R_Q to prevent quantum fluctuations of Q_0 ; simultaneously the resistor size should be small so that its stray capacitance does not significantly increase C_{Σ} . Experimental demonstration of the R-SET is still an unsolved problem despite significant progress in this direction [78,23]. Similar difficulty does not allow so far the experimental study of the so-called RC-SET [79] which would be very useful in digital circuits because of its multistable characteristics.

In contrast, C-SET was demonstrated repeatedly by many scientific groups using different materials and technologies (see Section II). In some laboratories it is a routine device which is used to measure very small charge variations, for example, in other single-electron circuits. The gate voltage U (see Fig. 2b) induces the effective charge into central island, $Q_0 \rightarrow Q_0 + C_g U$ (C_g is the gate capacitance), hence, Fig. 4 can be considered as a control curve of the C-SET. The gate voltage period is equal to $\Delta U = e/C_g$. If C_g is comparable to the junction capacitance, its contribution to the total capacitance should be also taken into account. To calculate characteristics of C-SET it is sufficient to use Eqs. (7)–(10) with the substitution $C_1 \rightarrow C_1 + \alpha C_g$, $C_2 \rightarrow C_2 + (1 - \alpha)C_g$, $Q_0 \rightarrow Q_0 + C_g U - \alpha C_g V$, where α is an arbitrary number (usually $\alpha = 0$ or $\alpha = 1$ is used).

If the resistances of two junctions of the C-SET are considerably different, then the I-V curve shows substantial periodic oscillations with period $\Delta V = e/C_1$ (for $R_1 \gg R_2$), called the Coulomb staircase. The cusps of the I-V curves shown in the inset of Fig.

3 correspond to condition $W_2 = 0$ in Eq. (8). Each period of staircase corresponds to an additional electron on the central island. Coulomb staircase is typical for experiments with the use of scanning tunneling microscope because the tunnel junction between its tip and conducting particle is typically much smaller than the junction between particle and substrate. In contrast, Coulomb staircase in C-SETs made of metal films is usually very weak, because this technology is able to produce junctions of the same parameters (in this case the staircase may be the evidence of a bad sample).

The theory of the SET-transistor is very well confirmed experimentally. Figure 5 shows the example of the layout, I-V curve, and the dependence of the current on the gate voltage for the C-SET made of metal films [25]. Unusually high operation temperature (up to 30 K) was achieved in this experiment by the use of the film anodization; typically metal film SETs operate at T < 4K so far. Simple "orthodox" theory described above is usually sufficient for the good quantitative agreement with experimental data for metallic C-SETs. Some additional factors should be typically taken into account for semiconductor C-SETs and double-junction structures with a molecule as the central island (see Section VI). Figure 6 shows the SEM image and the current – gate voltage dependence for the recently demonstrated Si-based SET [57] operable at the temperature over 80 K. The current in this device was actually carried by the tunneling holes, and the energy level spacing was comparable to the Coulomb blockade energy, that is why the authors of Ref. [57] call this device Single Hole Quantum Dot Transistor. Notice that the Coulomb oscillations in Fig. 6 are not exactly periodic and they are superimposed on the monotonic dependence on the gate voltage. We will discuss the reason for this difference from the behavior of metallic SETs in Section VI.

The C-SET can be used as a highly sensitive electrometer. The charge sensitivity of the SET-transistor is limited by its noise. In experiments the spectral density of this noise has usually 1/f dependence [20,24,27,80] that can be explained as the random capture of electrons by impurities in the tunnel barriers and/or the substrate in the vicinity of SET-transistor. The noise decreases with the improvement of the technology. The lower limit

is determined by the intrinsic thermal/shot noise of the SET-transistor [81,82] which was recently measured [83] at relatively high frequency where the contribution of 1/f noise is small. The ultimate sensitivity [81] limited by the intrinsic noise of the C-SET is given by $\delta Q_0 \approx 2.7e(k_BTC_\Sigma/e^2)^{1/2}(RC_\Sigma\Delta f)^{1/2}$ where Δf if the bandwidth. For typical parameters of the present day experiments, $C_\Sigma \sim 3 \times 10^{-16} F$, $T \sim 0.1 \text{K}$, $R \sim 10^5 \Omega$, the ultimate sensitivity is about $2 \times 10^{-6} e/\sqrt{Hz}$, while the best experimental sensitivity recorded so far is $7 \times 10^{-5} e/\sqrt{\text{Hz}}$ at 10 Hz [27].

Fitting of the experimental results obtained at T < 0.1 K usually shows that the real temperature is larger than the temperature of the cryostat. This can be explained as the heating due to the transport current [84,85,24] and imperfect microwave isolation of the SET-transistor from room-temperature environment.

The "orthodox" theory should be modified for the calculation of the small current well below the Coulomb blockade threshold at low temperatures. In this case the single electron tunneling is blocked, and the current is due to "simultaneous" tunneling (cotunneling) of two electrons through both junctions [74,75]. Because of the quantum nature of the process involving the whole electrical circuit, cotunneling is also called Macroscopic Quantum Tunneling of charge (q-MQT). The rate of such a process is proportional to the product $(R_Q/R_1)(R_Q/R_2)$, and, hence, is relatively small for $R_i \gg R_Q$.

V. DIGITAL SINGLE-ELECTRON DEVICES

The most important potential application of the single-electronics is the integrated digital electronics which could substitute conventional semiconductor transistor technology at the size scale below 30 nm. There have been many theoretical suggestions on this subject, we will discuss several of them.

A. Logic/memory using SET transistors

Conceptually the simplest way to realize digital single-electronics is to use SET-transistors instead of FET transistors in circuits resembling conventional electronics. It is possible to use capacitively coupled (C-SET) or resistively coupled (R-SET) transistors. Because R-SET is still too difficult for fabrication, let us limit the discussion to C-SET circuits.

For C-SET the dc input current is zero, hence, the power amplification is formally infinite. However, the voltage gain K_V is not large [12] (in contrast to semiconductor MOSFET transistors),

$$K_V \le C_g / \min(C_1, C_2). \tag{11}$$

The condition $K_V > 1$ which is necessary for the operation of logic devices requires the gate capacitance C_g to be larger than the junction capacitance.

The buffer/inverter can be realized by one SET-transistor in series with the load resistor R_L . Notice that the fabrication of such a resistor is not a big problem in contrast to the resistor for R-SET because there is no limitation on its stray capacitance. However, to reduce the number of technological steps, it is more reasonable to use a tunnel junction instead of the load resistor [86]. Calculations show [59] that for good operation of buffer/inverter, R_L should be at least 10 times larger than the junction resistance. Hence, the additional power dissipation in the load resistor will be much larger than that in SET-transistor.

To reduce the power consumption the complementary circuits can be used [12,58–60]. It is important that in contrast to CMOS technology in which n-MOS and p-MOS transistors are physically different, both complementary SET-transistors can be physically identical because of the periodic dependence of the current on the gate voltage. To achieve the complementary action, the operating point of one transistor should be on the raising branch of this dependence while for the other transistor it should be on the falling branch. It can be done with the use of additional capacitors [58] or different background charges in complementary transistors [59] (Fig. 7a). However, even without any special effort, complementary action occurs automatically in the simplest case of two symmetrical transistors with zero background charges [59]. It is interesting that in terms of the maximal operation temperature this simplest case is very close to the optimal one.

The maximal temperature at which the complementary inverter still amplifies the signal is equal to $0.026e^2/Ck_B$ [59] where C is the capacitance of one tunnel junction. Notice that the same maximal temperature can be obtained for resistively loaded transistor if R_L is very large. The maximal temperature is achieved when the gate capacitance C_g is about twice larger than the junction capacitance. The optimal C_g (corresponding to largest parameter margins) increases when the temperature decreases, so that $C_g/C \approx 3$ seems to be more or less the best choice for experimental realization. To have reasonable parameter margins, the temperature should be crudely twice less than the maximal temperature, $T \sim 0.01e^2/Ck_B$. In this case the margins for bias voltage and C_g are sufficiently wide (see Fig. 7b), and the critical margin is that for the fluctuations of background charges (about 0.1 e).

The operation point which optimizes the maximal temperature of the complementary inverter corresponds to relatively large power consumption about $2 \times 10^{-3} e^2/RC^2$ per SET-transistor. However, in the "power-saving" mode for a price of slight reduction of the operation temperature, the power consumption can be reduced down to $10^{-4}e^2/RC^2$ per transistor [59].

The switching time of the complementary inverter is close to $3RC_L$ where C_L is the load capacitance (see Fig. 7a). Relatively large load capacitance, $C_L \gtrsim 300C$, should be used in

order to make negligible the fluctuations of the output voltage due to the shot noise in the transistors.

Two inverters connected in a "circle" constitute the bistable flip-flop which can be used as a static memory cell. Almost all results of analysis of the inverter are directly applicable to the flip-flop. Slightly lower temperature and slightly narrower parameter margins are required for the operation of the logic gates based on SET-transistors [60]. A possible structure of the NOR gate [60] is shown in Fig. 8a. Notice that in contrast to SET inverter which is similar to the circuit used in conventional digital electronics, design of the SET NOR gate differs from the conventional one. (The direct reproduction of the design is impossible because of different characteristics of SET and MOSFET transistors.) The operation of SET NOR gate is illustrated in Fig. 8b. One can see that the threshold lines are close to the perfect (square) shape. Inversion of the bias voltage transforms NOR gate into NAND gate with the similar characteristics. NOR and NAND gates accompanied by the NOT gate (inverter) are more than sufficient for performing arbitrary logic functions. However, special design for some other gates, for example, SET XOR gate [60] can help to make the logic more efficient. The single-electron transformer Av-Kor-Naz can also be useful in the SET-transistor logic.

For a technology with a minimal feature size of 2 nm one can expect the capacitances of the tunnel junctions as low as 3×10^{-19} F. This corresponds to $e^2/Ck_B = 6 \times 10^3$ K; hence, the maximal temperature at which SET-transistor still amplifies the signal is close to 150 K. It would allow the operation of the SET logic at the liquid nitrogen temperatures. (We see that the room temperature operation requires the fabrication technology at sub-1 nm level.) For the estimate of the typical switching time let us take $R \approx 300k\Omega$ and $C_L \approx 10^3 C \approx 3 \times 10^{-16}$ F, then this time is about 1 ns. The power consumption per transistor is quite small, about 2×10^{-8} W for the parameters above in a typical operation point (in a "power saving operation point" it is about 10^{-9} W). However, because the density is very large, the power dissipation is a serious problem. For example, at 10^{11} transistors per cm² even in the power saving mode the total power is on the order of 100 W/cm^2 . Probably,

even more difficult problem of the logic/memory based on SET-transistors is the necessity to keep fluctuations of background charge within the margins on the order of 0.1e. This is a common problem for any integrated single-electronics, we will discuss the possible solutions in a separate subsection.

Let us emphasize that a single SET logic device can be relatively easy fabricated using the present-day technology. The multilayer technology which allows relatively large gate capacitances and solves the problem of connections between circuit elements has been already developed [88,27]. One can expect that first SET logic devices will be demonstrated within a few years (of course they will probably operate at T < 1 K and require individual adjustment of background charge at each island).

B. SEL logic and single-electron trap

In the logic/memory based on SET-transistors the logical unity and zero are represented by different dc voltage levels similar to how it is done in conventional digital electronics. Another possibility is to represent bits by single electrons [61–66], so that one extra electron in a conducting island would correspond to logical unity, while the absence of an extra electron, to logical zero. The circuits based on this truly single-electron approach are called Single-Electron Logic (SEL) [61–63]. The apparent advantage of this idea is a low power dissipation because in a static state there is no current, and the logical processing of one bit of information requires only few tunneling events.

In the initially proposed SEL logic [61] single electrons propagate together with information along the relatively long arrays of tunnel junctions and ohmic resistors. In this scheme the proper dc biasing is a difficult problem because the bias should be distributed in a specific way among the large number of cells. To resolve this problem it was suggested [62] to separate the propagation of electrons and information: electrons tunnel across the elementary cell which is a short biased array of junctions, while the information propagates from one cell to another perpendicular to the motion of electrons.

Fig. 9a shows the basic cell of the SEL family considered in Refs. [62–64]. Notice that it is similar to the complementary SET inverter, however, the important difference is that the capacitance of the middle island of a SEL cell is on the order of the junction capacitance (in contrast to large C_L in SET inverter). Inputs X and Y determine the charge state of the middle island. For example, if the lower branch of the cell is "closed" by the signal Y, and the signal X opens the upper branch of the cell, then one extra electron tunnels through the upper branch to the middle island. This creates the logical "unity". Parameters are chosen in a way that the next electron cannot come because of the increased potential of the island. The extra electron can be removed (creating logical "zero") from the middle island by closing the upper branch and opening the lower one. The charge of the middle electrode being the output of the cell, is used to affect the charge state of the next cell.

Figure 9b shows the SEL logical gate NOR. Signals X and Y are logical inputs. The middle island becomes charged by an extra electron when one of the upper branches opens. Clock signal T discharges the middle island at the end of the clock signal (upper branches should be closed at this time).

In contrast to the SET-transistor circuits, there is a strong back action from the output to the input in SEL circuits. Numerical simulations has proved [62–64] that the proper choice of parameters provides the unidirectionality of the signal propagation. However, because of the back action, the parameter margins are considerably narrower than in SET-logic case.

Another problem of SEL logic is that the information coded by a single electron can be destroyed by a single erroneous event due to cotunneling or thermoactivated tunneling. The possible solution would be the use of multijunction arrays as branches of SEL circuits, however, this possibility was not studied quantitatively yet.

The problems mentioned above make SEL logic circuits much more difficult to implement than SET-transistor logic at least at the present stage. However, one can hope that the problems will be eventually solved by the search of the optimal design and the improvement of the technology. This hope is strongly supported by a successful experimental demonstration [18,21,30] of the "memory cell" in which logical bit is represented by a single electron

on the conducting island.

This circuit which is usually called "single-electron trap", consists of several (typically, 5–7) tunnel junctions in series with a capacitor (Fig. 10a). Experimentally (Fig. 10b), this is an array of metal junctions which ends with a relatively large island so that its capacitance to the ground C_S is comparable to the junction capacitance C. The number of electrons on the island can be changed by application of the bias voltage U (Fig. 10a). Several charge states can be stable for the same U because of the Coulomb barrier created by the array of junctions. In the case of zero background charges the tunneling is blocked when $|V| < V_t = Ne/2C_{eff}$, $C_{eff} = C + ((N-1)/C + 1/C_S)^{-1}$ where V is the voltage across the array consisting of N junctions. One additional electron in the edge island changes V by $\Delta V = e/(C_S + C/N)$. Hence, as many as $m = 1 + \text{int}(2V_t/\Delta V)$ different states can be within the Coulomb blockade range. Two stable states (m = 2) which differ by one electron on the edge island represent logical unity and zero in a single-electron trap (Fig. 10c).

Similar to the SEL logic circuits, the erroneous switching of the single-electron trap are due to thermoactivated processes and cotunneling. Both processes are suppressed with the increase of the number of junctions in the array. The error rate less than 1 switching per 12 hours was demonstrated at the temperature of 50 mK in the 7-junction array made of aluminum tunnel junctions [30]. The charge state of the island was monitored with a help of near-by single-electron transistor (Fig. 10b). Theoretical consideration shows [89] that in principle the error rate below 10^{-17} s⁻¹ can be achieved in a similar trap.

If the capacitance C_S of the storage island is relatively large so that e/C_S is considerably smaller than the Coulomb blockade threshold V_t , then there are many, $m \approx 2V_t/(e/C_S)$, stable states within the blockade range. Representation of the logical bit by a single electron is ineffective in this case, however, the bit can be stored as several electrons on the island. For example, q = +me/2 can correspond to unity, and q = -me/2 corresponds to zero. The power dissipation during the writing process is larger than in single-electron case, however, for $m \sim 10$ –100 it is still extremely small. The advantage of the multi-electron storage is that single erroneous tunneling events do not destroy the information, and hence, the simple

refreshing of information can be used to avoid errors (in the single-electron case refreshing is possible only with the use of redundancy).

The multi-electron storage based on the Coulomb blockade was demonstrated [40] using a side-gated constriction in δ -doped layer of GaAs. The arrays of tunnel junctions appeared naturally in the constriction due to disorder. Several tens of electrons were used to represent a bit. The operation was confirmed up to the liquid helium temperature (4.2 K), and the storage time was as long as several hours.

The single-electron memory effects at room temperature were reported in silicon-based structures [53]. The current through the narrow ultrathin poli-Si film showed the hysteresis as a function of gate voltage. The effect was ascribed to the trapping of single electrons in small naturally formed grains of poli-Si. The use of disorder for the creation of extremely small islands (far beyond the limits of the modern lithography) offers the possibility of the high temperature operation. However, such a technique obviously has a problem with the reproducibility of sample characteristics because of the random nature of the island creation.

C. Wireless Single Electron Logic

Both SET-transistor circuits and SEL logic considered above require wires for the power supply and connections between circuit elements. Though the necessity of wires is not a principal problem, it is obviously inconvenient at the few-nanometer size scale. In the Wireless Single Electron Logic (sometimes the abbreviation WISE is used) proposed in Ref. [67] the power is supplied by alternating external electric field, and the capacitive coupling between neighboring cells is due to their close location. The "device" consists of many conducting islands, and the logical functions are determined by their specific arrangement (Fig. 11). Small "puddles" of 2D electron gas, small metallic droplets on an insulating substrate, or conducting clusters in a dielectric matrix are possible implementations of the islands. The basic cell of the logic is a short chain of closely located islands so that electrons can tunnel between neighboring islands. There is no tunneling between different chains

because of the larger separation.

Application of in-plane electric field E creates the voltage between the islands. When E exceeds the Coulomb blockade threshold E_t , the tunneling occurs somewhere inside the chain, producing an electron-hole pair. The electric field drags the components of the pair apart towards the opposite edges of the chain, creating the polarized state. If now the field E is decreased, the pair eventually annihilate, however, it will occur at the field E_a considerably smaller than E_t . Stability of both polarized and nonpolarized states for E between E_a and E_t allows to use these states as logical zero and unity.

The polarization change can propagate along a line of closely located chains (Fig. 11a). Suppose that all chains are not polarized initially, and E is slightly less than E_t . This is a metastable state. If one chain becomes polarized, the field of extra electron (hole) on the edge island increases the potential difference between neighboring islands of the next chain (Fig. 11a). This makes tunneling energetically favorable and leads to polarization of the next chain. This in turn polarizes the next chain and so on. The unidirectional propagation (in Fig. 11 from left to right) is a consequence of the asymmetry of the circuit.

The natural fan-out of the signal into two lines can be realized if both edge islands of a chain are used to trigger the next chains (Fig. 11b).

A "bi-controlled" chain (fifth from the right in Fig. 11c) which can be triggered by the polarization of either of two neighboring input chains can be used as the basic part of the logical gate OR. The logical gate AND can be designed similar to the OR gate, but with slightly larger distance between the "bi-controlled" chain and the neighboring input chains, in order to decrease their influence. Another possibility is to make the islands of "bi-controlled" chain slightly smaller in order to increase the Coulomb blockade energy.

Because of the asymmetry between logical zero and unity the design of the inverter is relatively complex. The circuit shown in Fig. 11d implements the logical function (NOT A).AND.B if the signal from input A comes before the signal from input B. This circuit can be used as NOT A, if logical unity always comes from input B and it comes later than signal A.

According to numerical simulations, the correct operation of the circuits shown in Fig. 11 requires that the magnitude of external field E lies within 5% margin [67]. This number gives also a crude estimate of the margins for other parameters (fluctuations of radius, spacing, etc.)

Considered logical gates together with propagation lines and fan-out circuits, are sufficient for computing. In the simplest mode of operation, all chains inside a device initially have zero polarization and external field is zero. Then external field increases up to a value for which all gates operate correctly, and cells start to switch in accordance with the input information flowing from the edges of the device. The result of the computation is the final polarization of output cells which can be read out, for example, by single-electron transistors. This simplest mode of operation can obviously be improved by the use of periodic changes of the external field ("clock cycles"). Properly chosen levels of the field can reset some cells but preserve the information in other cells.

Let us notice that the Wireless Single Electron Logic proposed in Ref. [67] somewhat resembles the earlier proposed Ground State Computing devices [90,91]. In both ideas the bistable polarization of the basic cell as well as only the nearest neighbor coupling are used. The main difference is the absence of the power supply in Ground State Computing, so that the only driving force is the fixed polarization of the cells at the "edges" of the device. The small total energy gain (proportional to the number of "edge" cells) should be distributed evenly between all "bulk" cells to ensure their deterministic sequential switching. Hence, an integrated Ground State Computing device cannot operate in the mode of sequential switching of cells. In order to reach the ground state, a significant part of the device should be involved in the macroscopic quantum process [74,75] ("simultaneous" switching of many cells), and this transition would require practically infinite time because of the exponential dependence on the number of cells. In contrast to the Ground State Computing, the principle of operation of the Wireless Single Electron Logic allows the traditional computing by the sequential switching of cells in the device of arbitrary large integration scale.

There is no static power dissipation in Wireless Single Electron Logic. Typically the

switching of a cell requires the energy of the order of only e^2/C where C is a typical capacitance. However, this dissipation can be further reduced. In the recent suggestion called Single Electron Parametron [68] the robust signal propagation along the shift register can cost even less, ultimately much less than k_BT per switching of a cell. The possibility of logic devices with the energy dissipation below thermal limit was proven long ago [92,93]. Single Electron Parametron seems to be the first realization of such a device based on the classical dynamics of the discrete internal degree of freedom.

The idea is shown in Fig. 12 (it represents the simplest, though not the best mode of operation). The basic cell is a chain consisting of 3 islands. Rotating electric field changes the polarization of the chain four times per period: islands are neutral (state "off") when the field is perpendicular to the plane of the chain, and chain is necessarily polarized (state "0" or "1") when the field is in-plain. When the neutral state becomes the polarized one, it can evolve into two different states: the electron from the central island can jump on either of two outer islands. The result is determined by the polarization of the neighboring (previous) chain which has became polarized earlier because of the change in the chain orientation along the propagation line. Notice that the next chain does not influence the decision because it is in a neutral phase at this time. The resulting polarization will in turn determine the polarization of the next chain when it will enter the polarized phase. For the circuit shown in Fig. 12 the signal propagation speed is 6 steps per period of field rotation, and the transmission rate is 2 bits per period, so on average each bit requires 3 chains.

The power dissipation less than k_BT per switching of a chain is achieved at low rotation frequency, $\omega \ll (k_BT)^2/e^3REd$, where R is the tunnel resistance and Ed is the voltage between islands induced by the in-plane component of the field. In this case the switching consists of the large number of electron jumps back and forth. In the adiabatic limit the energy $k_BT \ln 2$ is first taken from the thermostat (when neutral and polarized states have equal energies, the entropy is reduced by one bit) and then this energy is returned to the thermostat. In the first approximation the total power dissipation per switching is proportional to the switching speed.

In comparison with the Wireless logic of Ref. [67], Single-Electron Parametron offers also larger parameter margins [68]. Numerical simulations for a particular "layout" show the margin about 20% for the amplitude of the rotating electric field.

D. The problem of background charge

Fluctuating background charge is a very serious, possibly the most serious problem of the integrated single-electronics. Single-electron devices are so sensitive to the induced charge, that a single charged impurity in the close vicinity of a device can significantly influence its operation. In the case of a single circuit, background charges can be adjusted individually with a help of additional gates. There is obviously no such possibility for integrated circuits. What could be a solution of this problem?

First, the problem may turn out to be not so serious after all. There is some experimental evidence [9,14] that even in rather dirty systems the background charge tends to relax to zero. Theoretically this could be understood, for example, as being due to the attraction of the charged impurities to conducting surfaces by the image charge force. In general, one can hope that the narrow statistical distribution of background charges might occur naturally in some materials.

Second, it might be that the problem can be solved with the use of extremely pure materials. For example, if we speak about molecular electronic devices in which all circuit elements are reproducible on the atomic level, we can imagine extremely low concentration of impurities.

Third, instead of capacitively coupled single-electron devices we can try to use resistively coupled circuits. For example, R-SET transistor is not influenced by background charges at all. However, there are problems along this way. The R-SET is obviously much more difficult for fabrication than C-SET, and also the R-SET as a voltage amplifier requires significantly lower temperatures [94] because of the Nyquist noise in the coupling resistor.

Finally, one more possibility is to come up with some capacitively coupled devices which

would work in the environment of fluctuating background charges. The particular example of such a " Q_0 -independent device" was suggested recently [69].

The idea is to use C-SET in a mode when the ramping input signal drives the SETtransistor through several periods of its control characteristic. In this case the output signal will oscillate (Fig. 4), and for any initial Q_0 the amplitude of oscillation is equal to the maximal swing of the control characteristic. Such transistors can be used in a very-high density memory (10¹¹ bits/cm² or even more) to read out the stored information [69] (Fig. 13). Suppose that similar to traditional nonvolatile semiconductor memories [95], the digital bits are stored in a form of electric charge Q on the floating gate located in the vicinity of SET-transistor. In case of very small gate (of the order of 10 nm) this charge is just a few (10–20) electrons. The charge can be changed, for example, by its injection/extraction through the dielectric layer via Fowler-Nordheim tunneling [95] (the graded barrier would considerably improve the operation [69]). The cell is selected by the simultaneous application of the voltages of different polarity to word and bit lines (small voltage difference between two bit lines is used for the SET-transistor biasing – see Fig. 13). To read out the stored information we try to write the logical unity in. If unity has been already stored, the charge on the gate does not change, and the SET-transistor remains in the initial state. However, if logical zero has been stored on the gate, then its charge will gradually increase up to the level corresponding to logical unity. During this increase the current through SET-transistor oscillates that can be registered by a FET sense-amplifier (one FET may serve about 100 memory cells). The previously stored information is destroyed during read-out, hence, it should be restored later. Notice that voltage amplification by SET-transistor is not required in this mode of operation, and this fact significantly increases (by a factor ~ 5) the maximal operation temperature.

Estimates show [69] that the density of 10^{11} bits/cm² and the room temperature operation of such a memory is feasible for ~ 3 nm minimum feature size technology. Estimated read/write time is about 3 ns and is limited both by the time of the floating gate charging and by the intrinsic noise [81] of the SET-transistor.

Single-electron devices operating in Q_0 -independent mode seem to be the most radical solution of the problem of the background charge fluctuations. However, despite this idea can be used in the memory devices, it can be hardly applied to the logic circuits.

VI. SINGLE-ELECTRONICS IN SEMICONDUCTORS, CLUSTERS OF METAL ATOMS, AND MOLECULAR SYSTEMS

Single-electron effects become stronger with the decrease of the typical size. Besides that, they necessarily acquire new features. Eventually the field of single-electronics transforms into the field of atomic physics and chemistry; however, the basic ideas of single-electron devices are applicable even at this level. They can be used for the information processing in the hypothetical molecular electronics devices.

The "orthodox" theory works well for metallic systems down to crudely 1-nm size scale. At this scale the level discreteness in small metal particles (clusters of atoms) starts to play an important role. Besides that, increasing Coulomb energy becomes comparable to the height of the tunnel barriers leading to highly nonlinear I - V curves. In semiconductors these effects are important at considerably larger size scale and they are typical in experiments with quantum dots. Obviously, these effects should be also taken into account when the tunneling via single molecules is studied. That is why in this section we consider together the features of single-electron circuits based on semiconductor quantum dots, clusters of metal atoms and single molecules.

A. The level discreteness

The "orthodox" theory of single-electronics assumes the continuous energy spectrum of all electrodes. It should be somewhat modified [76,32,77] to take into account the level discreteness. As an example consider the SET-transistor with discrete spectrum of electrons in the central island. The complete description of the charge state now includes not only the total number of electrons on the island, but also the occupation of individual levels. In one-electron approximation (neglecting the collective excitations [96]) the electron addition energy depends on two integer parameters k and n:

$$E_{k,n} = \varepsilon_k + e(ne + Q_0 + e/2)/C_{\Sigma}, \tag{12}$$

where k is the level number (ε_k is the energy spectrum) and n is the total number of excess electrons on the island. Notice that the contribution from the background charge can be included into the definition of ε_k . The finite bias voltage can be taken into account in the same way as for the usual SET-transistor (Section IV). The tunneling rates should be calculated for each level individually. The rate of electron tunneling to/from the empty/occupied k-th level via j-th junction is given by expression

$$\Gamma = \Gamma_j \frac{1}{1 + \exp(-W/k_B T)}, \quad W = \pm (-1)^j \varepsilon_k \pm eV_j(n) - e^2/2C_{\Sigma},$$
(13)

where \pm stands for the direction of tunneling, $V_j(n)$ is the voltage drop across the junction given by Eq. (7), and Γ_j depends on the matrix element of tunneling and electron density in the external electrode (Γ_j can also depend on n and k). For the calculation of the average current and other characteristics Eq. (13) should be supplemented by some model describing the energy relaxation of the electrons on the island. Equations (5) and (8) of the "orthodox" theory can be obtained by summing Eq. (13) over all energy levels in the case of negligible level spacing, Fermi-distribution of electrons on the island, and constant Γ_j (then $R_j = \delta/e^2\Gamma_j$ where δ is the average level spacing).

The I-V curve of a SET-transistor with level discreteness contains the step-like features (Fig. 14a) which appear when the discrete level in the island crosses the Fermi level in external electrode. The position of the step along the voltage axis corresponds to W=0 in Eq. (13) and depends on two integer parameters k and n (in contrast to only one parameter n in usual SET-transistor) as well as on the junction number j. In the general case the arrangement of steps can be quite complicated, however, in typical cases the simple classification is possible. For example, Fig. 14a shows the I-V curve in the case when the level spacing δ (equidistant two-fold degenerate spectrum is assumed) is considerably less than the Coulomb energy e^2/C_{Σ} , and the barrier transparencies are significantly different. The level discreteness produces the fine structure superimposed on the Coulomb staircase. Notice that the level spacing contributes to the period of the Coulomb staircase, hence, there is no pure periodicity in the case of realistic nonequidistant spectrum ε_k . The slow energy

relaxation of the electrons on the island leads to some smoothing of the Coulomb staircase [76].

The discrete levels also modify the dependence of the current on the induced charge Q_0 . In this case it can have the multi-peak shape (compare Figs. 14b and 4). The slight asymmetry of the peaks in Fig. 14b is due to small difference between two tunnel barriers. The perfect periodicity is absent if the spectrum ε_k is not equidistant because it influences the position of the peaks. The level spacing δ contributes also to the average period making it larger than e.

In the "orthodox" theory the total number of conducting electrons on the island is large, so that it is possible to extract any number of them. This leads to some sort of electron"hole" symmetry. In the case of quantum dots or molecular-scale devices it is possible to have just few conducting electrons on the island, so that there is obviously no such a symmetry. Even the complete asymmetry when initially there are no conducting electrons on the island and they appear only due to transport, is quite typical (in semiconductors the same situation is also possible for holes). In this case the relative importance of the charge quantization and energy discreteness depends not only on the ratio $\delta/(e^2/C_{\Sigma})$ but also on the ratio Γ_e/Γ_c of emitter and collector barrier transparencies so that the actual parameter is $\alpha = \delta/(e/C_{\Sigma}) \times \Gamma_e/(\Gamma_e + \Gamma_c)$ [32]. For example, even if $(e/C_{\Sigma}) > \delta$ but the collector barrier is much lower so that $\alpha << 1$, than electrons do not accumulate on the central island, and steps on the I-V curve reflect only the spectrum ε_k . Coulomb staircase is noticeable only when $\alpha \gtrsim 1$.

Equations (12) and (13) are based on the classical expression $E_{int} = (me)^2/2C_{\Sigma}$ for the interaction energy of m electrons on the island. In the few-electron case (small m) the absence of the electrostatic self-interaction of an individual electron makes this simple expression considerably inaccurate, and the better approximation is $E_{int} = m(m-1)e^2/2C_{\Sigma}$ [76]. The good accuracy of this approximation is confirmed by exact calculation [97] of the interaction energy of few (up to 30) electrons on the sphere even in the extremely "quantum" case when electrostatic energy is much smaller than the Fermi energy.

The separation of the electrostatic and one-electron energy in Eq. (12) is definitely only a simple approximation, and in the exact theory the many-body problem should be solved. This problem is simplified in the case when only the low-temperature low-voltage conductance is studied, then the transport is determined by the ground states of the configurations with m and m+1 electrons on the island. The finite-voltage case requires also the calculation of excitations. There is some progress in this direction (see, e.g., Refs. [98,96]). However, the exact calculation is difficult not only because of the mathematical complexity of the problem, but also because the result is very sensitive to the geometry of the island which is usually not known accurately. The most widely used approximation is still Eq. (12), and it surprisingly well explains the experimental data (in some experiments the slow variation of the capacitance should be also taken into account – see next subsection).

The theory of single-electron transport in systems with discrete levels [76,32,77] was well confirmed experimentally both in metal and semiconductor structures. Let us discuss the difference of the typical parameters of these structures. First, let us estimate the energy level discreteness in a spherical cluster of aluminum atoms with diameter d=1 nm (it would contain only about 30 atoms). In the free electron gas approximation the average spacing δ (per spin) between levels is given by expression

$$\delta = \frac{1}{g(\varepsilon_F)v} = \frac{2\hbar^2 \pi^2}{v m (3\pi^2 \rho)^{1/3}},$$
(14)

where v is the volume, m is the effective electron mass, and ρ is the electron concentration. For the table value $\rho = 1.8 \times 10^{23} \text{ cm}^{-3}$ we obtain $\delta \approx 0.15 \text{ eV}$. Estimating the typical single-electron Coulomb energy, $\Delta = e^2/C_{\Sigma}$, let us take $C_{\Sigma} = \beta 2\pi\varepsilon\varepsilon_0 d$ with $\varepsilon \approx 5$ and the geometrical factor $\beta \approx 3$; then $E_c \approx 0.2 \text{ eV}$. We see that in metallic systems the level discreteness becomes comparable to the Coulomb energy roughly at 1-nm size scale, and the influence of the energy quantization is negligible when the typical size is larger than few nanometers. That is why the level discreteness is so difficult to observe in metallic single-electron devices.

The interplay between two effects in the metallic system was demonstrated experimen-

tally for the first time only recently [99] using the transport through a very small aluminum particle with volume about 130 nm³. The corresponding spacing was $\delta \approx 0.7$ meV while the charging energy was $\Delta \approx 12$ meV (the geometry was close to the plane capacitor that increased C_{Σ} in comparison with the estimate above). Because of the relatively small energy scale, the level discreteness showed up on the I-V curve only at the temperatures below 2 K (most measurements were done at T=0.3 K), at larger temperatures only Coulomb staircase was observed. Notice that the step-like features for the aluminum electrodes in the normal state were transformed in this experiment into the peak-like features [99] for superconducting electrodes because their shape directly corresponds to the density of states in electrodes.

The step-like features due to the level discreteness superimposed on the Coulomb stair-case were also observed in the experiment [51] with metal clusters $Pt_{309}Phen_{36}O_{30}$. The level spacing δ was up to 50 mV while the single-electron charging energy was up to 500 mV, and the discreteness was clearly observed at 4.2 K (the measurements at higher temperature were not reported in the paper). It is remarkable that the conducting particle used in this experiment can be described by the chemical formula (hence, formally this is a single molecule), and the "orthodox" theory (modified for the account of discreteness) is still very well applicable to this system. The experiments confirm that in metal systems the level discreteness is a small effect in comparison with single-electron charging effects when the size scale is larger than roughly 1 nm.

In the semiconductor systems the level discreteness becomes important at considerably larger size scale. This is caused by typically much lower electron concentration and lower effective electron mass (see Eq. (14)). For example, in Si-based systems with doping level $\rho \sim 10^{21} \text{ cm}^{-3}$, δ would become comparable to the Coulomb energy at $d \sim 5$ nm. For much lower doping concentration the interplay between the level discreteness and the Coulomb effects was reported [57] at $d \sim 20$ nm. The irregular position of the Coulomb oscillation peaks in Fig. 6 [57] can be ascribed to the irregular energy difference between neighboring discrete levels. Fluctuations of the peak height can be caused by the different tunneling

matrix elements for different levels.

A more dramatic increase of the level spacing occurs in semiconductor systems with twodimensional electron gas. In this case δ does not depend on the electron concentration, δ $\pi\hbar^2/2mS$, where S is the island area. Let us estimate electrical capacitance of the conducting island of 2D gas as $C_{\Sigma} = \varepsilon \varepsilon_0 S/a$. Here a is the effective distance from a conducting electrode in the plain capacitor geometry which is a good approximation when the "vertical" transport via quantum dot is studied. In the case of "lateral" transport (when conducting electrodes are in the same plain) this expression can be used with $a \sim 0.2d$ proportional to the diameter d of the dot. The ratio $\delta/(e^2/C_\Sigma)$ is equal to $\pi\hbar^2\varepsilon\varepsilon_0/2ma=a_B/2a$ where $a_B=4\pi\varepsilon\varepsilon_0\hbar^2/me^2$ is the Bohr radius in the given material. That is a natural result since by definition the Bohr radius corresponds to the length scale at which Coulomb and quantum energies coincide. In GaAs the Bohr radius is as large as 10 nm. This is why both the level discreteness and the single-electron effects are important [100,32,77] in experiments with electron transport through GaAs-based quantum dots [33-35,39,102-106] when the size scale a is comparable to 10 nm. Stressing the analogy with atomic physics in which the Bohr radius determines the size of the electron orbit, semiconductor quantum dots are sometimes called "artificial atoms" [5].

The relative importance of two effects is quite different in experiments with the vertical and lateral transport via quantum dots. In the vertical geometry a is close to the barrier width (in fact, the finite well width and the existence of two barriers should be taken into account [32]). The typical barrier width is 3–10 nm. Hence, the ratio $\delta/(e/C_{\Sigma})$ is typically on the order of unity, and even can be larger than unity. That is why the level discreteness is always important in the vertical transport via GaAs quantum dots and can be a major effect. In the first experimental study [101] of such a transport there was no sign of the single-electron charging effect, and the steps on the I-V curve were determined purely by the energy spectrum ε_k . That was because the collector barrier was much more transparent than the emitter barrier leading to $\alpha << 1$ (see discussion above). Similar experiment [33] with the increased thickness of the collector barrier showed the Coulomb staircase with

a fine structure due to ε_k . It was possible to change the major effect simply applying the different polarity of the voltage [33] because that interchanged the emitter and collector. The interplay between two effects in the vertical tunneling via quantum dot was also reported by several other groups (see, e.g., Refs. [102,103]).

In experiments with the lateral transport via a quantum dot, the single–electron charging energy is typically considerably larger than the level spacing. The estimate above gives for GaAs dot $\delta/(e^2/C_{\Sigma}) \sim 25 \text{nm}/d$, so that for the typical dot diameter $d \sim 0.5 \mu \text{m}$ this ratio is about 0.05 (this ratio somewhat increases if we take into account the capacitance increase due to the coupling to electrodes). Notice that the application of strong magnetic field changes the energy spectrum and can considerably increase the level spacing δ .

There were many experiments demonstrating the coexistence of the energy and charge quantizations in the lateral transport via a quantum dot. Let us mention several of them [34,35,39,104-106] and the recent review [107] on this topic. Figure 15a shows the experimental I-V curve with the Coulomb staircase and the fine structure due to the level discreteness [104]. The inset shows the layout of the metal gates which form the quantum dot in the two-dimensional electron gas beneath them. The dependence of the current on the voltage of the central gate C is shown in Fig. 15b. This gate does not affect much the tunnel barriers but changes the induced charge in the dot. The multi-peak shape of the dependence is the consequence of the level discreteness (compare with Fig. 14b).

The theory described above can be also applied to the tunneling through single molecules. Experimental I-V curves in such systems [47–50] typically have a region of Coulomb blockade and cusps or steps resembling Coulomb staircase, and these features are usually discussed in terms of single-electron transport. If the molecule contains the relatively large cluster of metal atoms (see, e.g., Ref. [51]), the good agreement even with the simple "orthodox" theory can be expected. However, if the cluster consists of just few atoms or there is no metal cluster at all, the theory of single-electronics should be used with some caution. First of all, the level discreteness is not a small correction in this case but a major factor. Typically the separation of the Coulomb energy and one-electron spectrum assumed in Eq. (12) should

fail, and the excitation spectrum should considerably depend on the charge number n. The calculation of capacitances could be used only for crude estimates and typically there should be no symmetry between addition and removal of electrons (electron affinity and ionization energy can be quite different) leading to highly asymmetric I-V curves. In contrast to "orthodox" theory, it can be impossible to add or remove more than 2–3 electrons to/from a molecule without its mechanical breakdown or chemical transformation. Thus, the experimental results in the single-molecule systems can considerably differ from the predictions of the standard theory of single-electronics.

On the other hand, it is surprising that such macroscopic quantity as the capacitance can be sometimes used even at the microscopic size scale. In the model considered in Ref. [97] only a few conducting electrons are sufficient to establish a well-defined capacitance (the formal definition fluctuate only slightly with the number of electrons). As a curious example let us mention that the first three ionization energies of the single aluminum atom (5.97 eV, 18.8 eV, and 28.5 eV [108]) correspond to the dimensionless sequence 1: 3.1: 4.8 which is very close to the "orthodox" sequence 1: 3: 5.

B. Barrier dependence on the voltage

In the previous subsection the single-electron charging energy e^2/C of the 1-nm aluminum grain was estimated as 0.2 eV. This number can be comparable to the energy height H of the tunnel barrier which depends on the material and is typically between 0.3 eV (thermally grown aluminum oxide) and 3 eV (vacuum barrier). This would lead to highly nonlinear I-V curves of single-electron devices.

If the barrier has low transparency then the typical voltage of the I-V curve nonlinearity is even much less than H/e and is comparable to $\hbar/e\tau$ where τ is the traversal time of tunneling (in case of the rectangular barrier $\tau = l/(2H/m)^{1/2}$ where l is the barrier width). For example, if H = 1 eV and l = 2 nm, then $\hbar/e\tau = 0.2$ eV.

Hence, the finite height of the barrier becomes an important factor [1,109,110] in metallic

single-electron devices typically at the size scale of 1 nm (in some materials it appears considerably earlier [80]). The suppression of the tunnel barrier by the applied voltage is always the strong effect in experiments with lateral transport via semiconductor quantum dots because of typically low barrier height. For example, Fig. 15a shows the experimental I - V curves [104] in which the voltage scale of the exponential nonlinearity of the I - V curve is comparable to the period of the Coulomb staircase. Notice that in semiconductor devices the barrier suppression is typically important even when the relatively large size scale does not allow to resolve individual levels. Finite barrier height is obviously also important in the single-molecule systems because of large typical voltages.

The effect can be taken into account within "orthodox" theory (neglecting for simplicity the level discreteness) by introduction of the nonlinear "seed" I - V curve $I_0(V)$ of the tunnel junction [1]. The tunneling rates in this case are given by the general expression

$$\Gamma = \frac{I_0(W/e)}{e(1 - \exp(-W/k_B T))} \tag{15}$$

instead of Eq. (5) (W is the energy gain due to tunneling). A more accurate approximation [111,112] takes into account the change of the image charge potential due to Coulomb blockade and gives the additional factor $\exp(e^2\tau/12C\hbar)$.

When the nonlinearity of $I_0(V)$ is relatively small at the single-electron voltage scale $V \sim e/C$ (it implies $\hbar/\tau \ll e^2/C$), the I-V curve of the SET-transistor preserves usual Coulomb features. However, the current grows exponentially with voltage, so that it becomes impossible to measure experimentally the offset voltage, and the Coulomb staircase becomes smoother [109] (see Fig. 15a [104]). In case of strong nonlinearity (which is not yet achieved experimentally) Coulomb staircase should completely disappear and give place to the new periodic features with different period [109].

Let us mention one more effect which is important in semiconductor single-electron devices. In contrast to metallic systems, the geometrical size of a semiconductor conducting island can depend on the number of electrons on the island and on the gate voltage. Hence, the capacitance is not constant, leading to nonperiodicity of the Coulomb staircase and

the nonperiodic dependence on the gate voltage in SET-transistor. The change of the geometric size also leads to the change of the width of a tunnel barrier while the barrier height can be directly affected by the gate voltage. Sufficiently large gate voltage can either completely deplete the conducting island or remove the tunnel barrier depending on the polarity. As a consequence, on the large scale of the gate voltage semiconductor SET-transistors usually behave like FET transistors (see Figs. 6 and 15b): starting from the state with negligible current, one can finish with the perfectly open transport channel. Single-electron quasiperiodic dependence on the gate voltage (Coulomb oscillations) is observed in relatively narrow range of the gate voltage when the conducting island has already appeared but the tunnel resistance of the barrier is still larger than the quantum unit R_Q .

VII. CONCLUSION

We have considered only a part of issues related to the field of single-electronics. For example, we did not mention single-electron effects in superconducting systems [1], including the possibility to measure experimentally the parity of the total number of electrons in superconducting islands [19,113]. Another interesting subject is the single-electron oscillations with the frequency determined by the dc current, f = I/e [1,71,78,23,114,115]. This relation can be inverted: the magnitude of the dc current can be accurately controlled by the frequency of applied ac bias [15–17] that is used in single-electron turnstile [16] and pump [17]. We have not discussed also the problem of cotunneling [74,75], the effect of the electromagnetic environment [72,73], photon-assisted tunneling [116–118], coherent effects [119,120], and many other issues.

Single-electronics was a rapidly growing field during the last ten years, and this growth still continues. It is already clear that single-electronics is interesting not only from the scientific point of view, but it can be really used in applications. The simplest application is the use of the SET-transistor for various purposes as a very sensitive electrometer capable to measure sub-electron charges. Another clear application is the standard of dc current [29] based on the single-electron pump. It is quite possible that arrays of small tunnel junctions will be used as low-temperature thermometers [22]. Other applications are definitely coming.

The most important potential application is the ultradense (up to 10¹² cells per cm²) integrated digital electronics which was the main topic of the present review. The question if such a prospect is real, is still quite uncertain because of very difficult problems on this way. The main problem is the necessity of the new technology capable to deal with objects on the order of 1 nm or even less. This length scale is imposed by the requirement of the room-temperature operation. It is likely that such a technology should use conducting clusters of atoms embedded in the molecular matrix, hence, we speak about the molecular electronics devices. Another major obstacle on the way to integrated single-electronics is the random distribution of the background charge. If the technology will not offer the solution of this

problem, only circuits operating in Q_0 -independent mode [69] will be practical, and this will considerably limit the variety of possible devices.

Despite the problems, the ultradense integrated single-electronic circuits will hopefully be eventually realized and will be able to substitute the CMOS technology to continue the exponential growth of the computer performance. The rapid progress in experimental single-electronics, in particular, the recent demonstration of the devices operating at the temperature of liquid nitrogen and even at room temperature, strongly supports this hope.

The author thanks D. V. Averin and K. K. Likharev for the numerous discussions and the critical reading of the manuscript. The author is also grateful to Y. Nakamura, E. Leobandung, P. D. Dresselhaus, and A. T. Johnson for providing figures with experimental results. The work was supported in part by ONR grant No. N00014-93-1-0880 and AFOSR grant No. 91-0445.

REFERENCES

- D. V. Averin and K. K. Likharev, in *Mesoscopic Phenomena in Solids*, edited by B.
 L. Altshuler, P. A. Lee, and R. A. Webb (Elsevier, Amsterdam, 1991), p. 173.
- [2] K. K. Likharev, IBM J. Res. Dev. 32, 144 (1988).
- [3] Single Charge Tunneling, edited by H. Grabert and M. H. Devoret (Plenum, New York, 1992).
- [4] K. K. Likharev and T. Claeson, Scientific American 266, 50 (1992).
- [5] M. A. Kastner, Phys. Today **46**, No. 1, 24 (1993).
- [6] C. J. Gorter, Physica **15**, 777 (1951).
- [7] C. A. Neugebauer and M. B. Webb, J. Appl. Phys. **33**, 74 (1962).
- [8] I. Giaver and H. R. Zeller, Phys. Rev. **181**, 789 (1969).
- [9] J. Lambe and R. C. Jaklevic, Phys. Rev. Lett. **20**, 1504 (1969).
- [10] I. O. Kulik and R. I. Shekhter, Sov. Phys. JETP 41, 308 (1975).
- [11] D. V. Averin and K. K. Likharev, J. Low Temp. Phys. **62**, 345 (1986).
- [12] K. K. Likharev, IEEE Trans. on Magn. 23, 1142 (1987).
- [13] T. A. Fulton and G. C. Dolan, Phys. Rev. Lett. **59**, 109 (1987).
- [14] L. S. Kuzmin and K. K. Likharev, JETP Lett. 45, 496 (1987).
- [15] P. Delsing, K. K. Likharev, L. S. Kuzmin, and T. Claeson, Phys. Rev. Lett. 63, 1861 (1989).
- [16] L. J. Geerligs, V. F. Anderegg, P. A. M. Holweg, J. E. Mooij, H. Pothier, D. Esteve,C. Urbina, and M. H. Devoret, Phys. Rev. Lett. 64, 2691 (1990).
- [17] H. Pothier, P. Lafarge, R. F. Orfila, C. Urbina, D. Esteve, and M. H. Devoret, Physica

- B **169**, 573 (1991).
- [18] T. A. Fulton, P. L. Gammel, and L. N. Dunklleberger, Phys. Rev. Lett. **67**, 3148 (1991).
- [19] M. T. Tuominen, J. M. Hergenrother, T. S. Tighe, and M. Tinkham, Phys. Rev. Lett. 69, 1997 (1992).
- [20] G. Zimmerli, T. M. Eilies, R. L. Kautz, and J. M. Martinis, Appl. Phys. Lett. 61, 237 (1992).
- [21] P. LaFarge, P. Joyez, H. Pothier, A. Cleland, T. Holst, D. Esteve, C. Urbina, and M. H. Devoret, C.R. Acad.Sci. Paris, Ser. II, 314, 883 (1992).
- [22] J. P. Pekola, K. P. Hirvi, J. P. Kauppinen, and M. A. Paalanen, Phys. Rev. Lett. 73, 2903 (1994).
- [23] L. S. Kuzmin and Yu. A. Pashkin, Physica B 194-196, 1713 (1994).
- [24] S. M. Verbrugh, M. L. Benhamadi, E. H. Visscher, and J. E. Mooij, J. Appl. Phys. 78, 2830 (1995).
- [25] Y. Nakamura, D. L. Klein, and J. S. Tsai, Appl. Phys. Lett. 68, 275 (1996).
- [26] P. Wahlgren, P. Delsing, D. B. Haviland, Phys. Rev. B 52, 2293 (1995).
- [27] E. N. Visscher, S. M. Verbrugh, J. Lindeman, P. Hadley, and J. E. Mooij, Appl. Phys. Lett. 66, 305 (1995).
- [28] K. P. Hirvi, J. P Kauppunen, A. N. Korotkov, M. A. Paalanen, and J. P. Pekola, Appl. Phys. Lett. 67, 2096 (1995).
- [29] J. M. Martinis, M. Nahum, and H. D. Jensen, Phys. Rev. Lett. 72, 904 (1994).
- [30] P. D. Dresselhaus, L. Ji, S. Han, J. E. Lukens, and K. K. Likharev, Phys. Rev. Lett. 72, 3226 (1994).

- [31] U. Meirav, M. A. Kastner, and S. J. Wind, Phys. Rev. Lett. 65, 771 (1990).
- [32] A. N. Korotkov, D. V. Averin, and K. K. Likharev, Physica B 165, 927 (1990); D.
 V. Averin, A. N. Korotkov, and K. K. Likharev, Phys. Rev. B 44, 6199 (1991).
- [33] Bo Su, V. J. Goldman, and J. E. Cunningham, Science 255, 313 (1992).
- [34] P. L. McEuen, E. B. Foxman, U. Meirav, M. A. Kastner, Y. Meir, N. S. Wingreen, and S. J. Wind, Phys. Rev. Lett. 66, 1926 (1991).
- [35] N. C. van der Vaart, S. F. Godijn, Y. V. Nazarov, C. J. P. M. Harmans, J. E. Mooij, L. W. Molenkamp, and C. T. Foxon, Phys. Rev. Lett. 74, 4702 (1995).
- [36] C. I. Duruöz, R. M. Clarke, C. M. Marcus, and J. S. Harris, Jr., Phys. Rev. Lett. 74, 3237 (1995).
- [37] F. R. Waugh, M. H. Berry, D. J. Mar, R. M. Westervelt, K. L. Campman, and A. C. Gossard, Phys. Rev. Lett. 75, 705 (1995).
- [38] L. P. Kouwenhoven, S. Jauhar, J. Orenstein, P. L. McEuen, Y. Nagamune, J. Motohisa, and H. Sakaki, Phys. Rev. Lett. 73, 3443 (1994).
- [39] O. Klein, C. de C. Chamon, D. Tang, D. M. Abusch-Magder, U. Meirav, X.-G. Wen, and M. A. Kastner, Phys. Rev. Lett. 74, 785 (1995).
- [40] K. Nakazato, R. J. Blaikie, and H. Ahmed, J. Appl. Phys. 75, 5123 (1994).
- [41] P. J. M. van Bentum, R. T. M. Smokers, and H. van Kempen, Phys. Rev. Lett. 60, 2543 (1988).
- [42] R. Wilkins, E. Ben-Jacob, and R. C. Jacklevic, Phys. Rev. Lett. 63, 801 (1989).
- [43] J.-C. Wan, K. A. McGreer, N. Anand, E. Nowak, and A. M. Goldman, Phys. Rev. B 42, 5604 (1990).
- [44] A. E. Hanna and M. Tinkham, Phys. Rev. B 44, 5919 (1991).

- [45] C. Schönenberger, H. van Houten, and H. C. Donkersloot, Europhys. Lett. **20**, 249 (1992).
- [46] M. Dorogi, J. Gomes, R. Osifchin, R. P. Andres, R. Reifenberger, Phys. Rev. B 52, 9071 (1995).
- [47] H. Nejoh, Nature **353**, 640 (1991).
- [48] H. Nejoh, M. Ueda, and M. Aono, Jpn. J. Appl. Phys (Part 1), 32, 1480 (1993).
- [49] C. M. Fischer, M. Burghard, S. Roth, and K. v. Klitzing, Europhys. Lett. 28, 129 (1994).
- [50] A. A. Zubilov, S. P. Gubin, A. N. Korotkov, A. G. Nikolaev, E. S. Soldatov, V. V. Hanin, G. B. Khomutov, and S. Ya. Yakovenko, Tech. Phys. Lett. 20, 195 (1994).
- [51] J. G. A. Dubois, J. W. Gerritsen, S. E. Shafranjuk, E. J. G. Boon, G. Schmid, and H. van Kempen, "Coulomb staircase and quantum size effects in tunneling spectroscopy on ligand stabilized metal clusters", preprint (1995).
- [52] K. Matsumoto, M. Ishii, K. Segawa, Y. Oka, B. J. Vartanian, and J. S. Harris, Appl. Phys. Lett. 68, 34 (1996).
- [53] K. Yano, T. Ishii, T. Hashimoto, T. Kobayashi, F. Murai, and K. Seki, IEEE Trans. on Electron. Dev. 41, 1628 (1994).
- [54] Y. Takahashi, M. Nagase, H. Namatsu, K. Kurihara, K. Iwdate, Y. Nakajima, S. Horiguchi, K. Mirase, and M. Tabe, Electron. Lett. 31, No. 2, 136 (1995).
- [55] A. Fujiwara, Y. Takahashi, K. Mirase, and M. Tabe, Appl. Phys. Lett. **67**, 2957 (1995).
- [56] H. Matsuoka and S. Kimura, Appl. Phys. Lett., 66, 613 (1995).
- [57] E. Leobandung, L. Guo, Y. Wang, and S. Y. Chou, Appl. Phys. Lett. 67, 938 (1995);Appl. Phys. Lett. 67, 2339 (1995).

- [58] J. R. Tucker, J. Appl. Phys. **72**, 43339 (1992).
- [59] A. N. Korotkov, R. H. Chen, and K. K. Likharev, J. Appl. Phys. 78, 2520 (1995).
- [60] R. H. Chen, A. N. Korotkov, and K. K. Likharev, "Single-electron-transistor logic", to be published.
- [61] K. K. Likharev and V. K. Semenov, in Extended Abstracts of International Superconductive Electronics Conference, Tokyo, 1987, p. 182.
- [62] K. K. Likharev, S. F. Polonsky, and S. V. Vyshenskii, "Single-electron logic/memory family", (unpublished, 1990).
- [63] D. V. Averin and K. K. Likharev, in Ref. [3], p. 311.
- [64] Yu. V. Nazarov and S. V. Vyshenskii, in Single-Electron Tunneling and Mesoscopic Devices, edited by H. Koch and H. Lubbig (Springer, Berlin, 1992), p. 61.
- [65] K. Nakazato and J. D. White, IEDM 1992, 487 (1992).
- [66] M. G. Ancona, J. Appl. Phys. **79**, 526 (1996).
- [67] A. N. Korotkov, Appl. Phys. Lett., 67, 2412 (1995).
- [68] K. K. Likharev and A. N. Korotkov, "Single-electron parametron", in: *Proceedings of IWCE'95* (Tempe, AZ), to be published.
- [69] K. K. Likharev and A. N. Korotkov, "Ultradense hybrid SET/FET dynamic RAM: feasibility of background-charge-independent room-temperature single-electron digital circuits", in: *Proceedings of ISDRS'95 (Charlottesville, Virginia)*, to be published.
- [70] E. H. Hauge and J. A. Støvneng, Rev. Mod. Phys., 61, 917 (1989).
- [71] N. S. Bakhvalov, G. S. Kazacha, K. K. Likharev, and S. I. Serduykova, IEEE Trans. Magn. 25, 1436 (1989).
- [72] Yu. V. Nazarov, JETP Lett. 49, 126 (1989).

- [73] G.-L. Ingold and Yu. V. Nazarov, in Ref. [3], p. 21.
- [74] D. V. Averin and A. A. Odintsov, Phys. Lett. A **140**, 251 (1989).
- [75] D. V. Averin and Yu. V. Nazarov, in Ref. [3], p. 217.
- [76] D. V. Averin and A. N. Korotkov, Sov. Phys. JETP, 70, 937 (1990); J. Low Temp. Phys. 80, 173 (1990); in: *Molecular Electronics*, ed. by P. I. Lazarev (Kluwer, Netherlands, 1991), p. 9.
- [77] C. W. J. Beenakker, Phys. Rev. B 44, 1646 (1991); H. van Houten, C. W. J. Beenakker, and A. A. M. Staring, in Ref. [3].
- [78] L. S. Kuzmin, D. B. Haviland, Phys. Rev. Lett. 67, 2890 (1991).
- [79] A. N. Korotkov, Phys. Rev. B 49, 16518 (1994).
- [80] Yu. A. Pashkin, L. S. Kuzmin, A. N. Tavkhelidze, F.-J. Ahlers, T. Weimann, D. Quenter, and J. Niemeyer, "All-chromium single electron tunneling transistor", to be published.
- [81] A. N. Korotkov, D. V. Averin, K. K. Likharev, and S. V. Vasenko, in Single-electron tunneling and mesoscopic devices, ed. by H. Koch and H. Lubbig (Springer, Berlin 1992), p. 45; A. N. Korotkov, Ph. D. Theses (Moscow State University, 1991); Phys. Rev. B 49, 10381 (1994).
- [82] S. Hershfield, J. H. Davies, P. Hyldgaard, C. J. Stanton, and J. W. Wilkins, Phys. Rev. B 47, 1967 (1993).
- [83] H. Birk, M. J. M de Jong, and C. Schönenberger, Phys. Rev. Lett. **75**, 1610 (1995).
- [84] R. L. Kautz, G. Zimmerli, and J. M. Martinis, J. Appl. Phys. **73**, 2386 (1993).
- [85] A. N. Korotkov, M. R. Samuelsen, and S. A. Vasenko, J. Appl. Phys. 76, 3623 (1994).
- [86] H. Fukui, M. Fujishima, and K. Hoh, in: Ext. Abstracts, ICSSD'94 (Yokohama, 1994),

- p. 331.
- [87] D. V. Averin, A. N. Korotkov, and Yu. V. Nazarov, Phys. Rev. Lett. 66, 2818 (1991).
- [88] G. Zimmerli, R. L. Kautz, and J. M. Martinis, Appl. Phys. Lett. 61, 2616 (1992).
- [89] L. R. C. Fonseca, A. N. Korotkov, K. K. Likharev, and A. A. Odintsov, J. Appl. Phys. 78, 3238 (1995).
- [90] C. S. Lent, P. D. Tougaw, W. Porod, and G. H. Bernstein, Nanotechnology 4, 49 (1993).
- [91] S. Bandyopadhyay, B. Das, and A. E. Miller, Nanotechnology 5, 113 (1994).
- [92] C. Bennett, IBM J. Res. Devel. 17, 525 (1973).
- [93] K. K. Likharev, Int. J. Theor. Phys. **21**, 311 (1982).
- [94] A. N. Korotkov, "Resistively coupled SET", in preparation.
- [95] Nonvolatile Semiconductor Memories, ed. by C. Hu, (IEEE, New York, 1991).
- [96] D. Weinmann, W. Häusler, and B. Kramer, Phys. Rev. Lett. 74, 984 (1995).
- [97] L. Belkhir, Phys. Rev. B **50**, 8885 (1994).
- [98] D. Jovanovic and J.-P. Leburton, Phys. Rev. B 49, 7474 (1994).
- [99] D. C. Ralph, C. T. Black, and M. Tinkham, Phys. Rev. Lett. 74, 3241 (1995).
- [100] A. Groshev, Phys. Rev. B **42**, 5895 (1990).
- [101] M. A. Reed, J. N. Randall, R. J. Aggarval, R. J. Matyi, T. M. Moore, and A. E. Wetsel, Phys. Rev. Lett. 60, 535 (1988).
- [102] P. Guéret, N. Blank, R. Germann, and H. Rothiizen, Phys. Rev. Lett. 68, 1896 (1992).
- [103] M. Tewordt, V. J. Law, J. T. Nicholls, L. Martín-Moreno, D. A. Ritchie, M. J. Kelly, M. Pepper, J. E. F. Frost, R. Newbury, and G. A. C. Jones, Solid-State Electronics

- **37**, 793 (1994).
- [104] A. T. Johnson, L. P. Kouwenhoven, W. de Jong, N. C. van der Vaart, C. J. P. M. Harmans, and C. T. Foxon, Phys. Rev. Lett. 69, 1592 (1992).
- [105] E. B. Foxman, P. L. McEuen, U. Meirav, N. S. Wingreen, Y. Meir, P. A. Belk, N. R. Belk, M. A. Kastner, and S. J. Wind, Phys. Rev. B 47, 10020 (1993).
- [106] J. Weis, R. J. Haug, K. von Klitzing, and K. Ploog, Semicond. Sci. Technol. 9, 1890 (1994).
- [107] L. P. Kouwenhoven and P. L. McEuen, "Single electron transport through a quantum dot", to be published in: *Nano-Science and Technology* (ed. by G. Timp).
- [108] Landolt-Börnstein, Numerical data (Springer, Berlin, 1950), vol. I/1, p. 211.
- [109] A. N. Korotkov, Yu. V. Nazarov, Physica B 173, 217 (1991).
- [110] M. T. Lutwyche and Y. Wada, J. Appl. Phys. **75**, 3654 (1994).
- [111] A. N. Korotkov, Phys. Rev. B 49, 11508 (1994).
- [112] D. V. Averin, Phys. Rev. B **50**, 8934 (1994).
- [113] D. V. Averin and Yu. V. Nazarov, Phys. Rev. Lett. **69**, 1993 (1992).
- [114] A. N. Korotkov, D. V. Averin, and K. K. Likharev, Phys. Rev. B 49, 1915 (1994).
- [115] A. N. Korotkov, Phys. Rev. B **50**, 17674 (1994).
- [116] K. K. Likharev and I. A. Devyatov, Physica B **194-196**, 1341 (1994).
- [117] C. Bruder and H. Schoeller, Phys. Rev. Lett. **72**, 1076 (1994).
- [118] L. P. Kouwenhoven, S. Jauhar, J. Orenstein, P. L. McEuen, Y. Nagamune, J. Motohisa, and H. Sakaki, Phys. Rev. Lett. 73, 3443 (1994).
- [119] A. Yacoby, M. Heiblum, D. Mahalu, and H. Shtrikman, Phys. Rev. Lett. 74, 4047

(1995).

[120] M. Büttiker and C. A. Stafford, Phys. Rev. Lett. **76**, 495 (1996).

FIGURES

- FIG. 1. (a) Schematic energy diagram of the tunnel junction and (b) the tunneling rates Γ^+ and Γ^- for both directions as functions of the voltage V across the junction. The Coulomb blockade suppresses the tunneling at $|V| < e/2C_{eff}$ (solid lines). The cusps of the curves are rounded due to finite temperature. The dashed lines show Γ^+ and Γ^- for the case without single-electron effects $(e/C_{eff} = 0)$.
- FIG. 2. Single-electron transistor (SET): (a) the basic part consisting of two tunnel junctions in series, (b) capacitively coupled SET (C-SET), and (c) resistively-coupled SET (R-SET). The current through the SET depends on the subelectron fraction of the charge Q_0 .
- FIG. 3. The typical I-V curves for the symmetrical SET and the SET with different resistances of junctions (inset) calculated using Eqs. (5)–(10) for different Q_0 .
- FIG. 4. The typical theoretical dependence of the current through the symmetrical SET on the induced charge Q_0 for different bias voltages V.
- FIG. 5. Experimental realization [25] of the C-SET using narrow metal films: (a) layout, (b) I-V curves for different gate voltages and (c) the dependence of the current on the gate voltage at different temperatures (courtesy of Y. Nakamura). The curves in (b) and (c) are shifted vertically for clarity.
- FIG. 6. Si-based SET-transistor [57]: electron micrograph of the structure and the dependence of the current on the gate voltage (courtesy of E. Leobandung). The current is actually due to the hole tunneling, so the structure is named Single Hole Quantum Dot Transistor.
- FIG. 7. (a) The complementary inverter made of two SET-transistors and (b) its parameter window for different temperatures [59].

FIG. 8. (a) The NOR gate made of SET-transistors and (b) its typical output characteristics on the plane of input signal amplitudes [60]. The solid lines in (b) show the "active" region where the output cannot be definitely interpreted, and the areas between solid and dashed lines correspond to the noise margins.

FIG. 9. The basic cell of the SEL logic and (b) the SEL NOR gate [62–64].

FIG. 10. The single-electron trap: (a) schematic drawing, (b) the electron micrograph of the structure and (c) the hysteretic dependence of the trapped charge (multiplied by the coupling coefficient) on the voltage $U = V_{trap}$ [30] (courtesy of P. D. Dresselhaus). The charge is measured by the SET-transistor (upper part of the layout). The height of each loop in (c) corresponds to one extra electron in the trap.

FIG. 11. "Wireless" Single-Electron Logic [67] based on tunneling between small conducting islands and biased by electric field E. (a) The propagation line, (b) the circuit for fan-out, (c) the logical gate OR (gate AND has a similar design), and (d) the gate (NOT A). AND. B which can be used as an inverter.

FIG. 12. Shift register of the Single-Electron Parametron [68]. Information propagation is caused by the rotating electric field E(t).

FIG. 13. Ultradense hybrid SET/FET memory operating in Q_0 -independent mode [69].

FIG. 14. (a) The typical I-V curve and (b) the typical $I-Q_0$ dependence calculated for the SET-transistor with discrete spectrum of the central island. Fine structure in (a) is due to the level spacing δ while the Coulomb staircase is determined mainly by the Coulomb energy $\Delta = e^2/C_{\Sigma}$. The $I-Q_0$ dependence can have the multi-peak shape in contrast to usual SET (see Fig. 4).

FIG. 15. (a) The experimental I-V curve and (b) the dependence of the current on the gate voltage [104] for the C-SET based on the GaAs quantum dot (courtesy of A. T. Johnson). Notice the fine structure on the I-V curve and the multi-peak shape of curves in (b) due to the level discreteness. Also notice the nonlinearity of the I-V curve because of the barrier suppression.

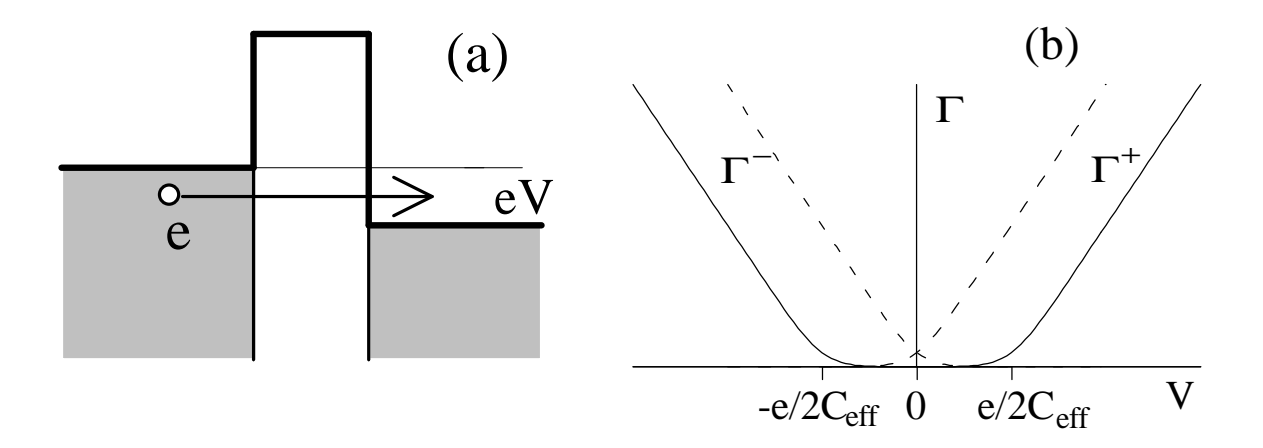


Fig. 1

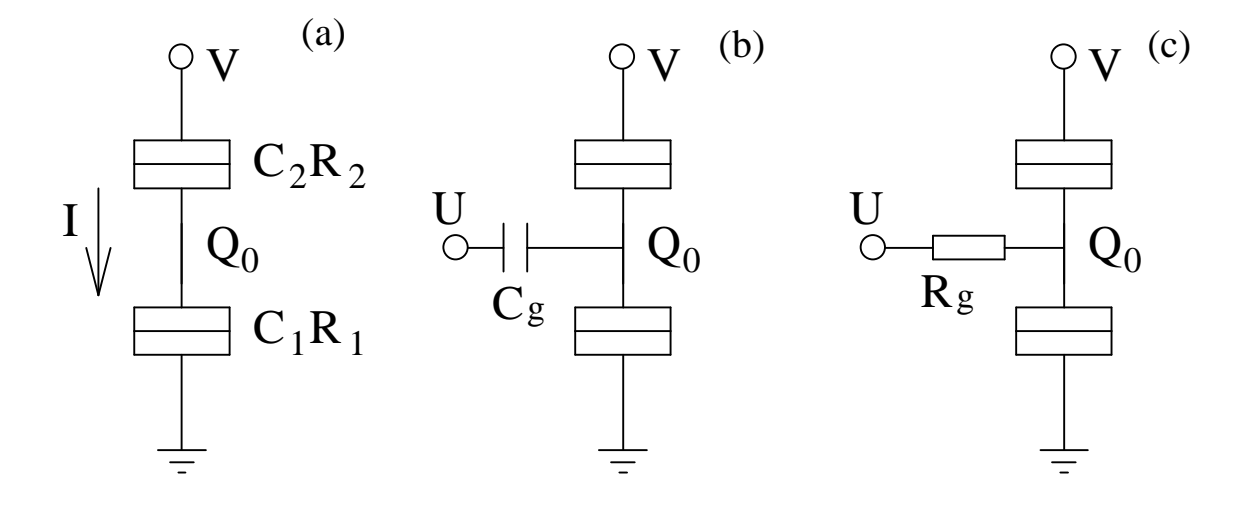


Fig. 2.

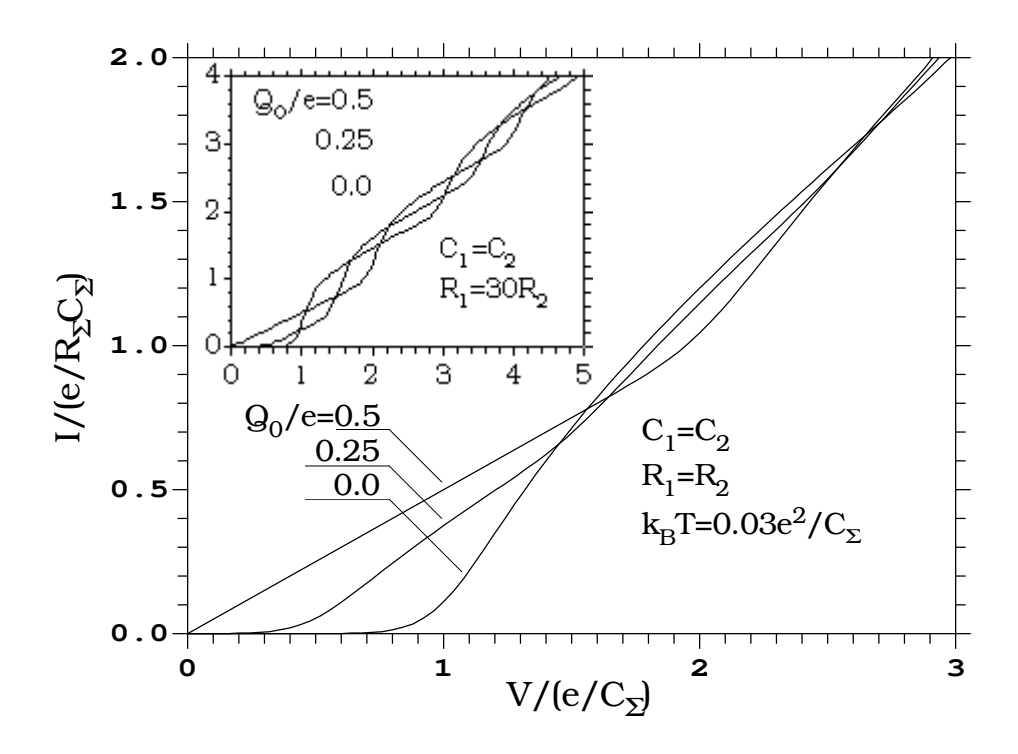


Fig. 3

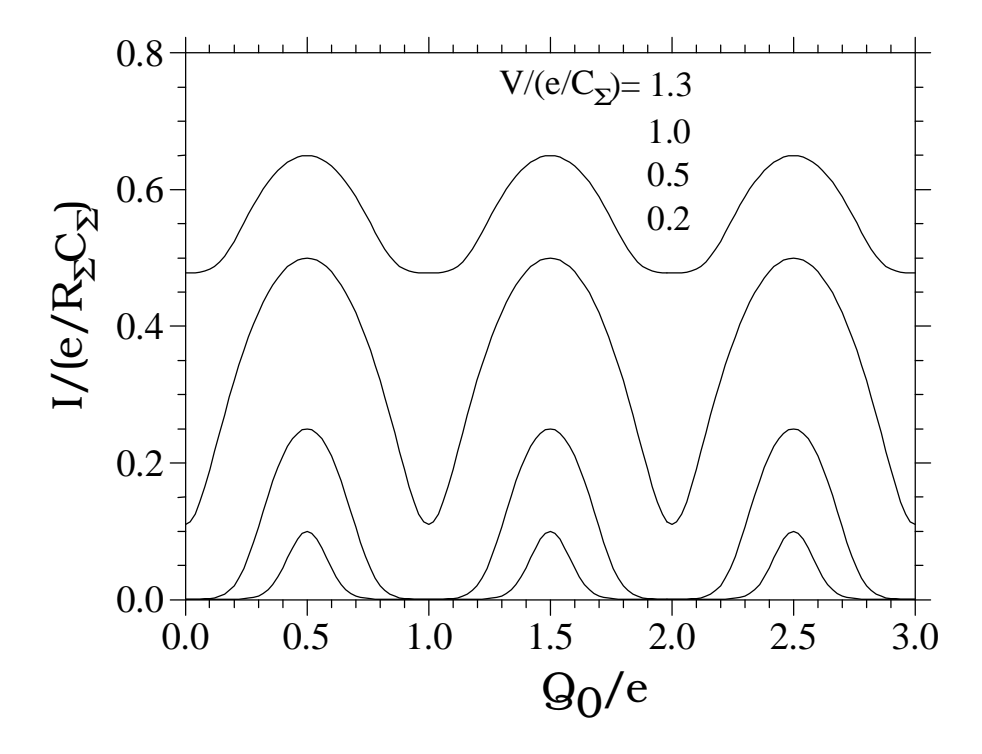
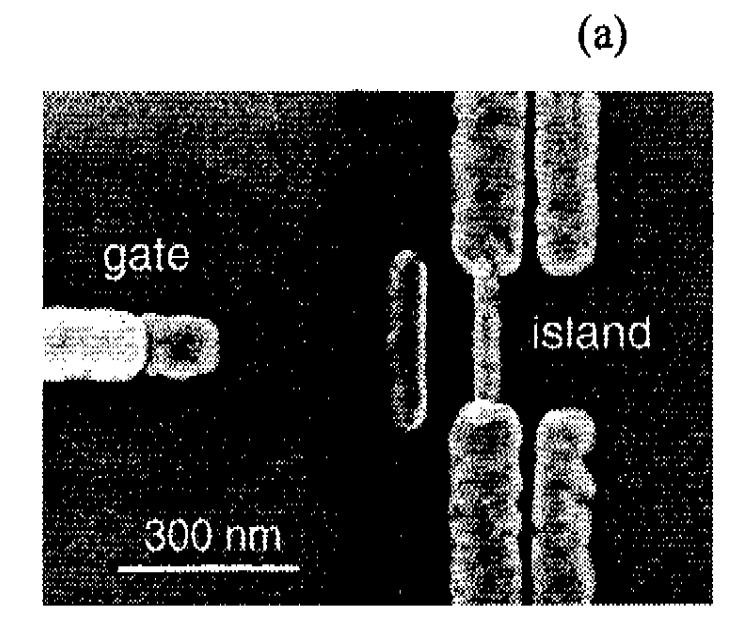


Fig. 4



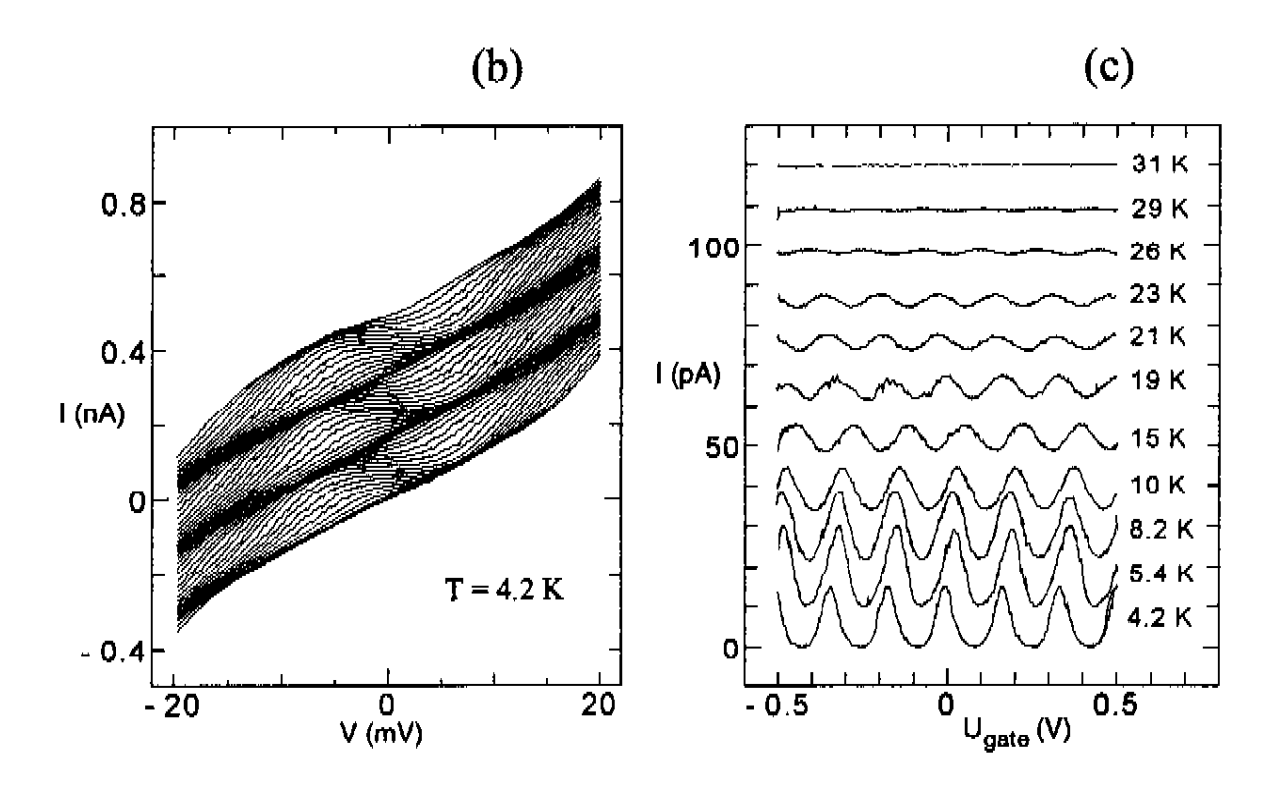


Fig. 5

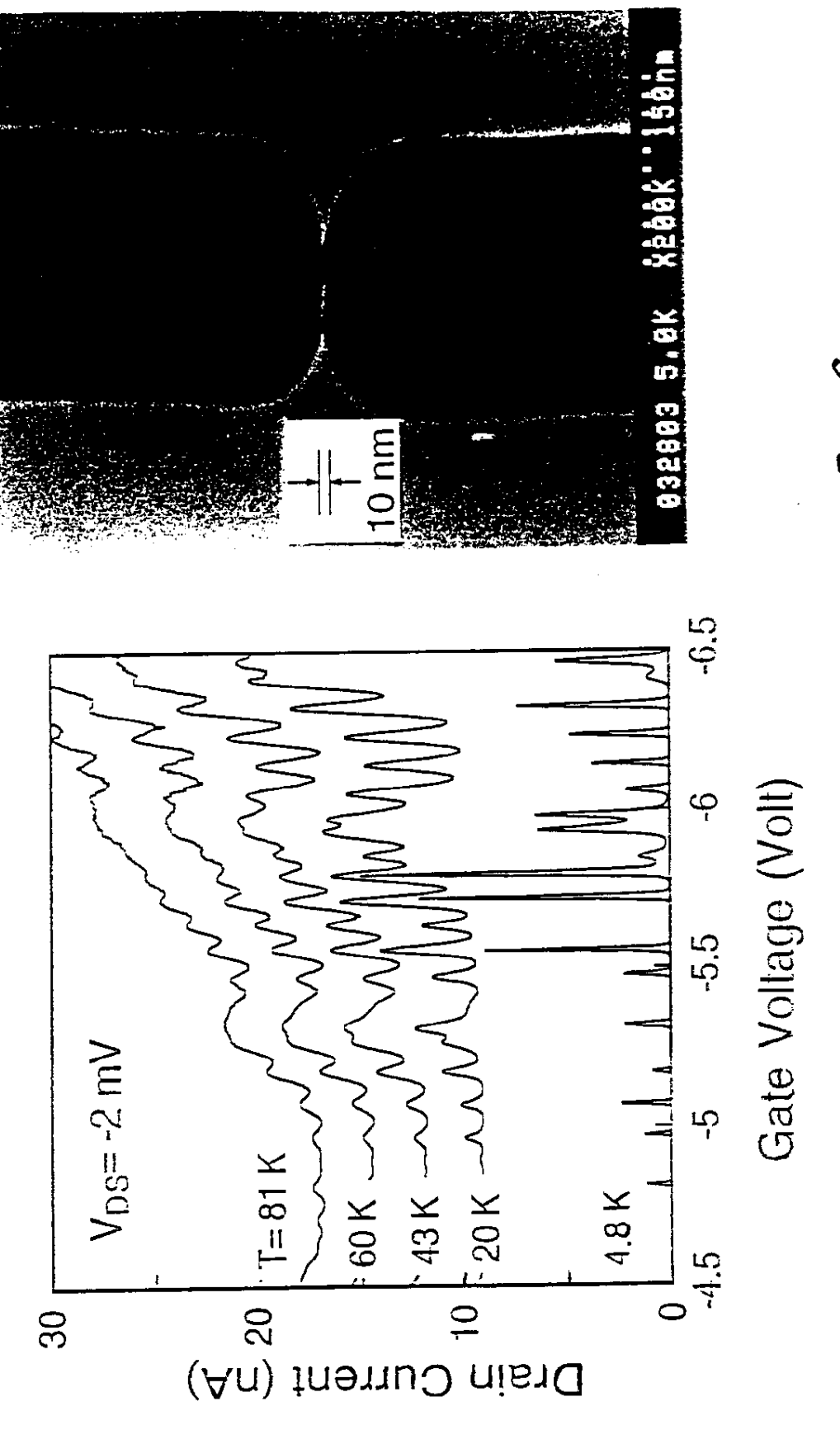
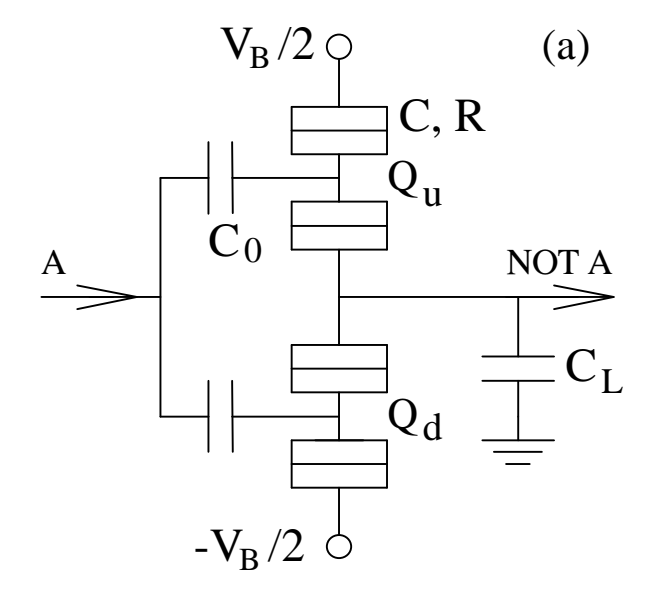


Fig. 6



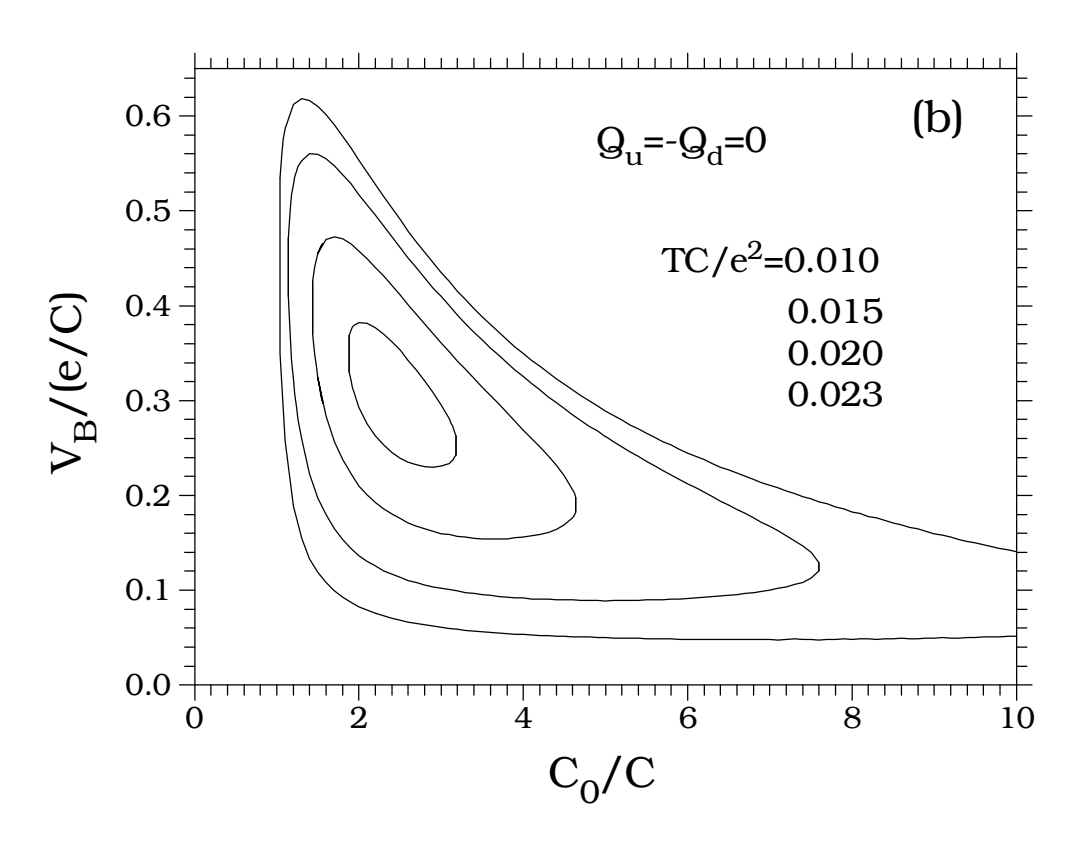
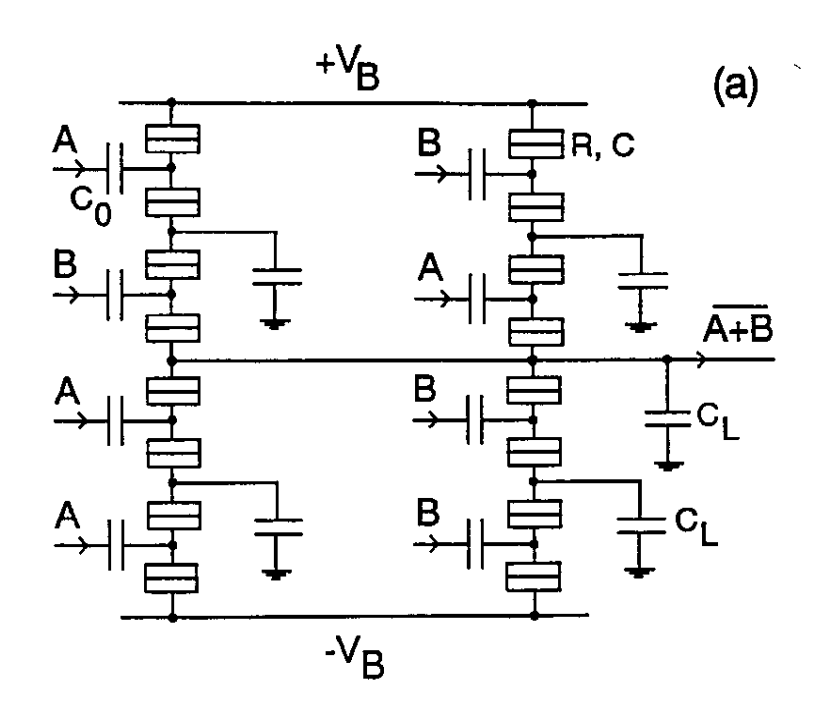


Fig. 7



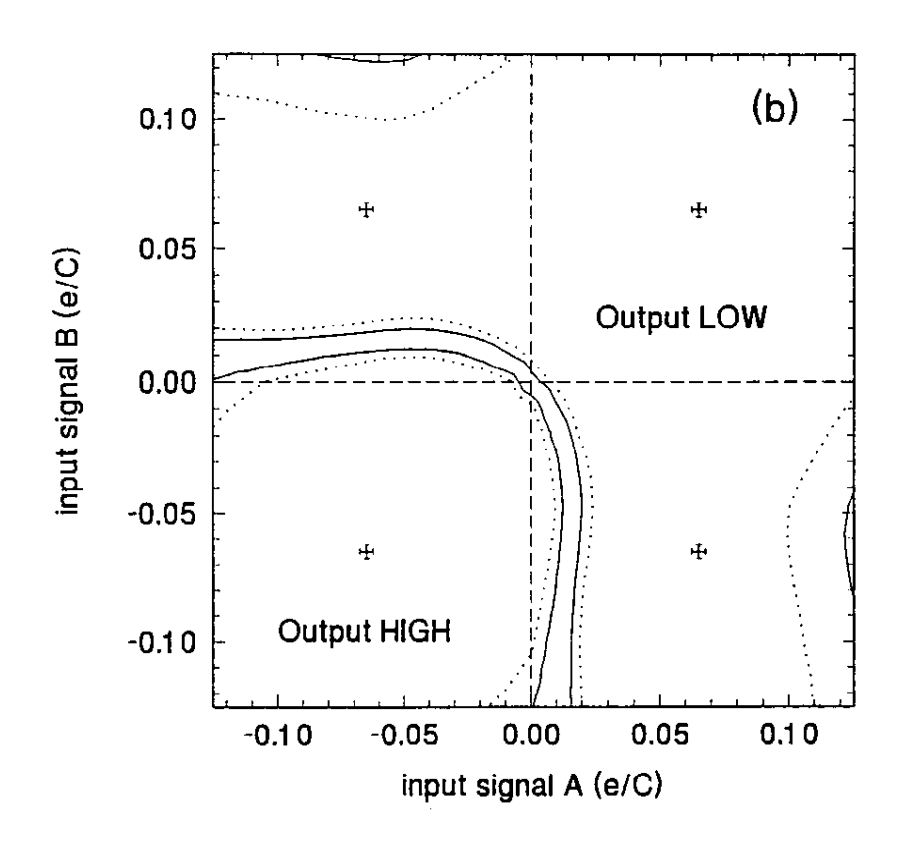


Fig. 8

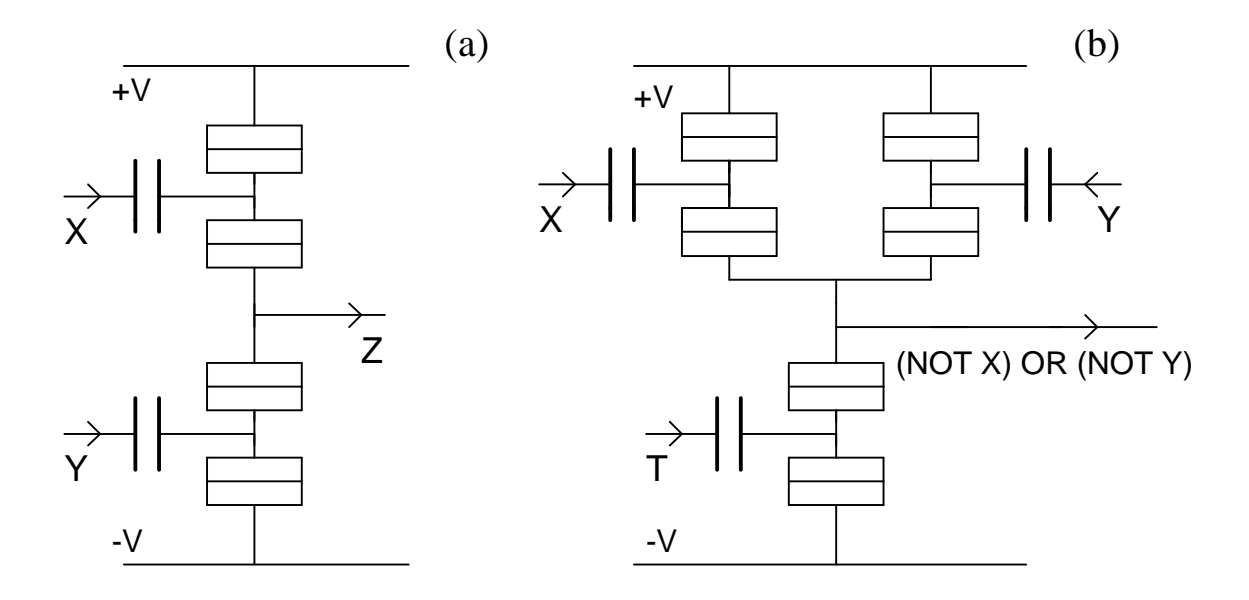
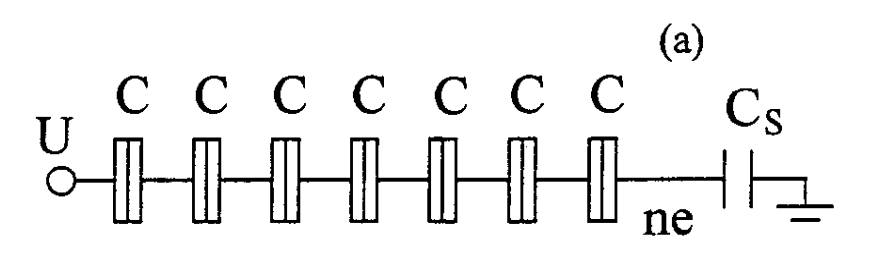
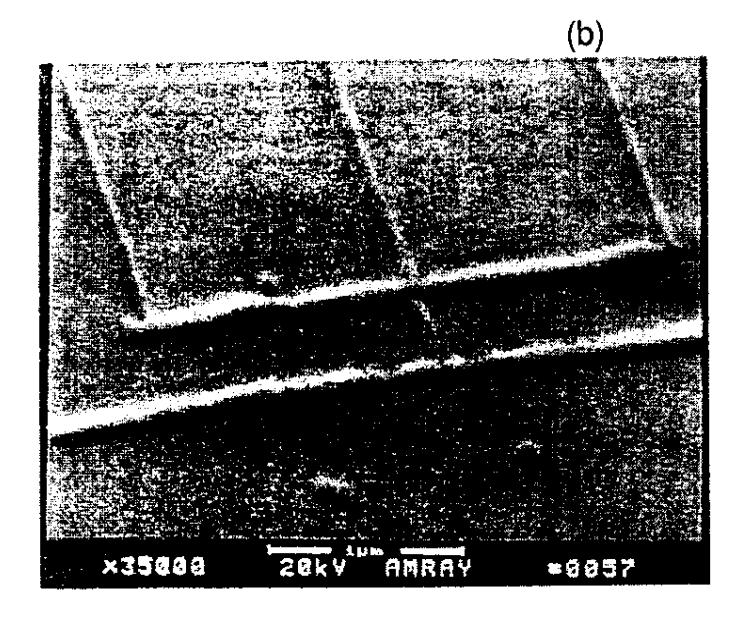


Fig. 9.





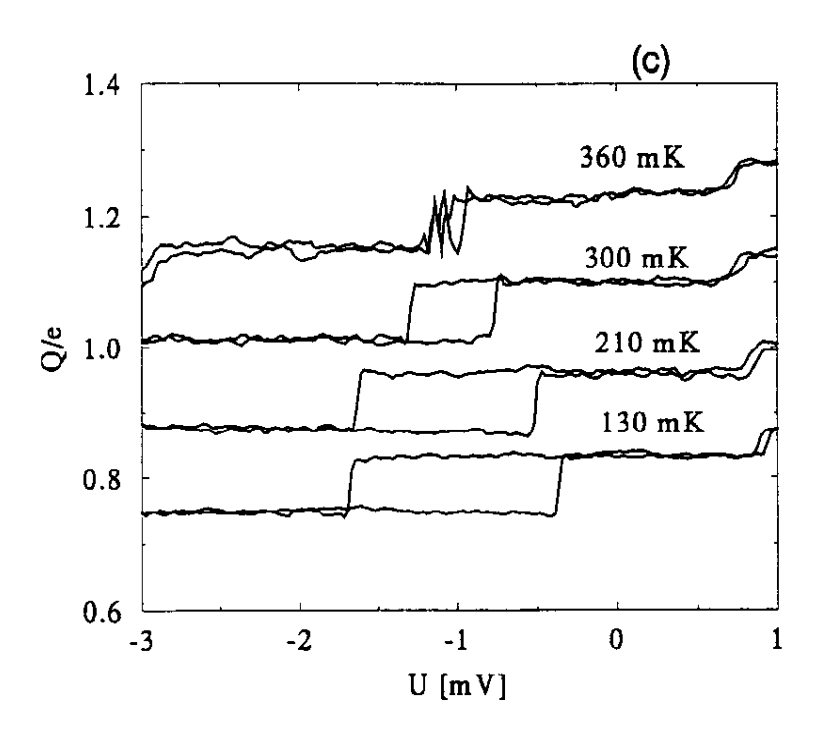


Fig. 10

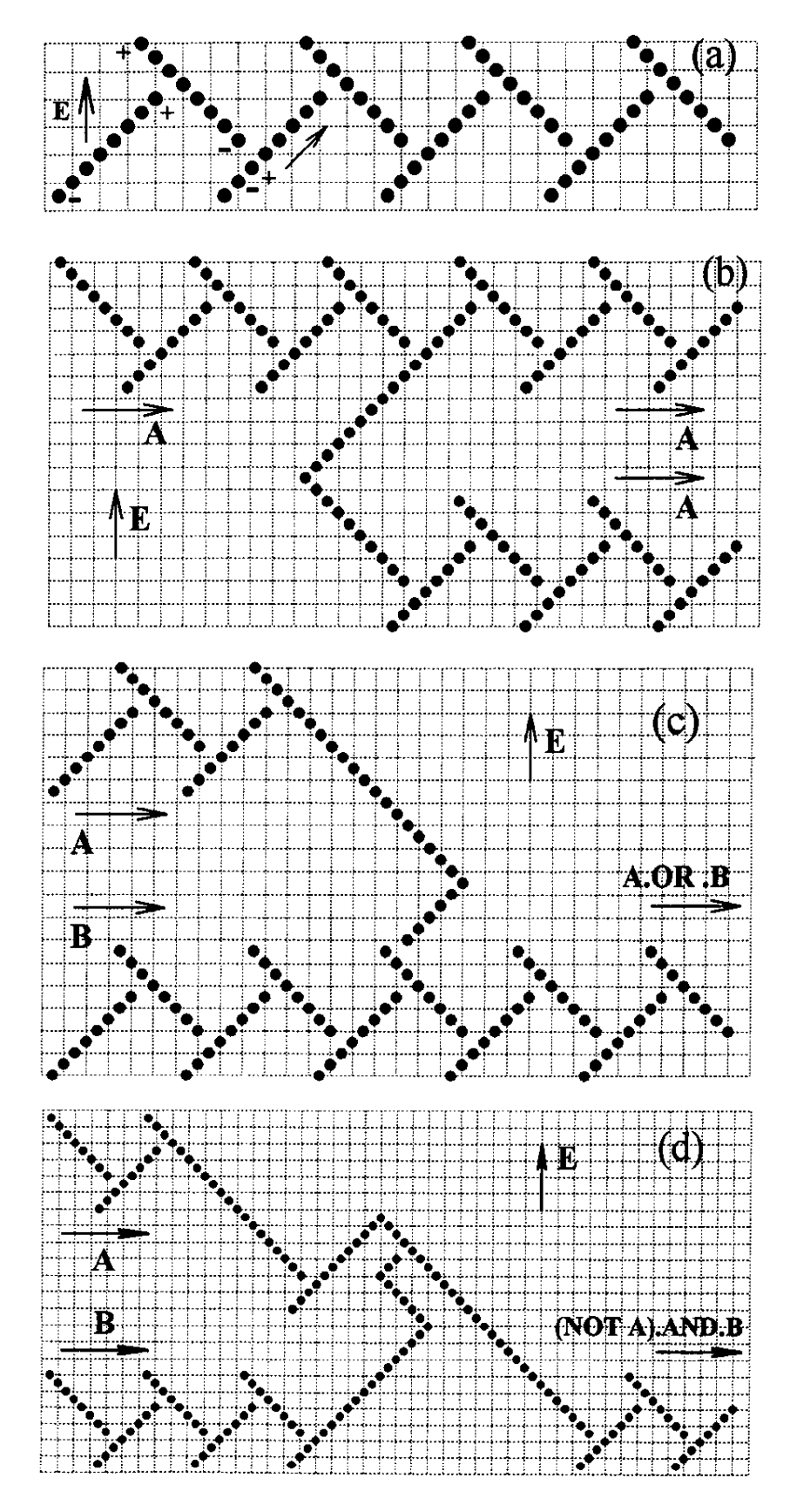


Fig. 11

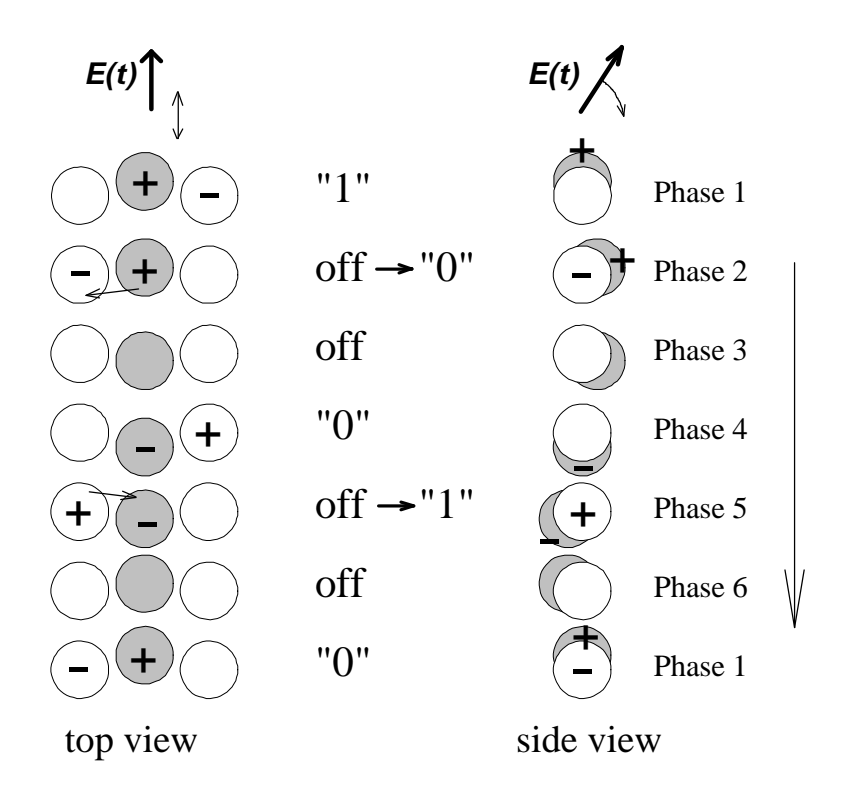


Fig. 12

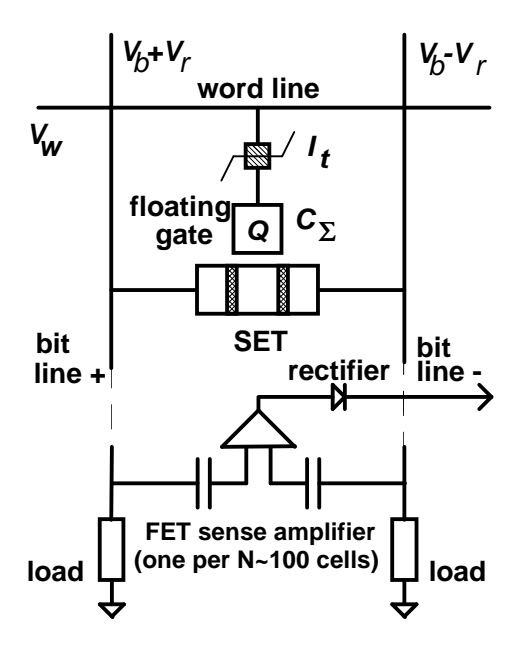
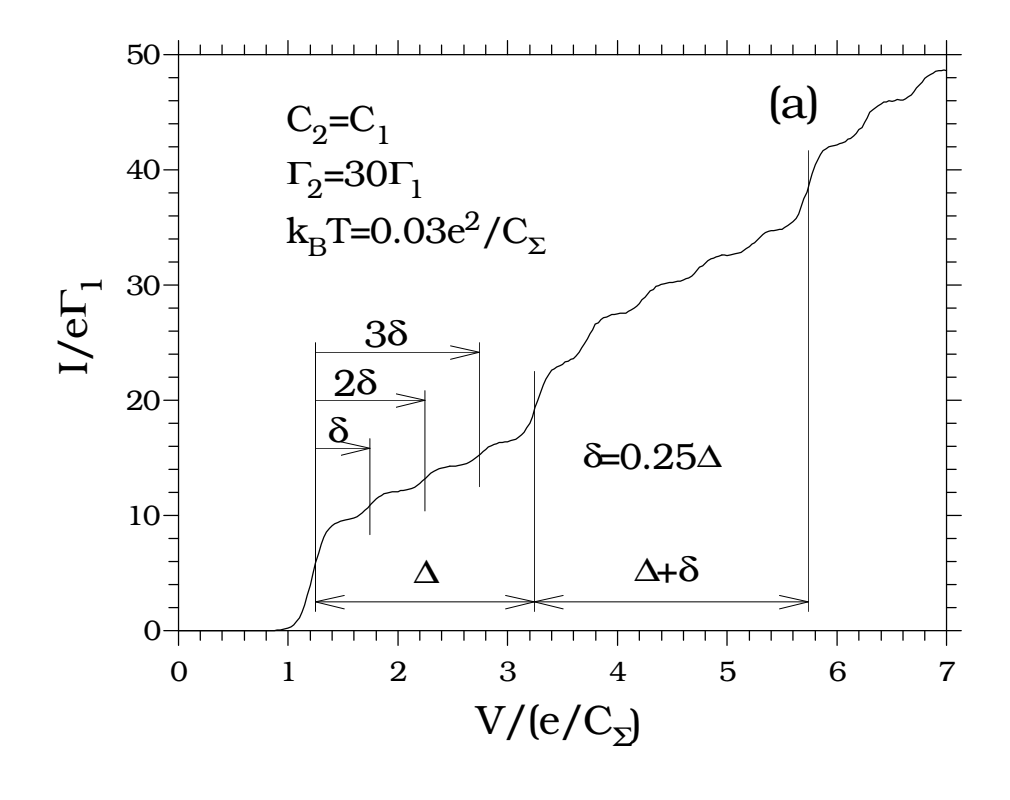


Fig. 13



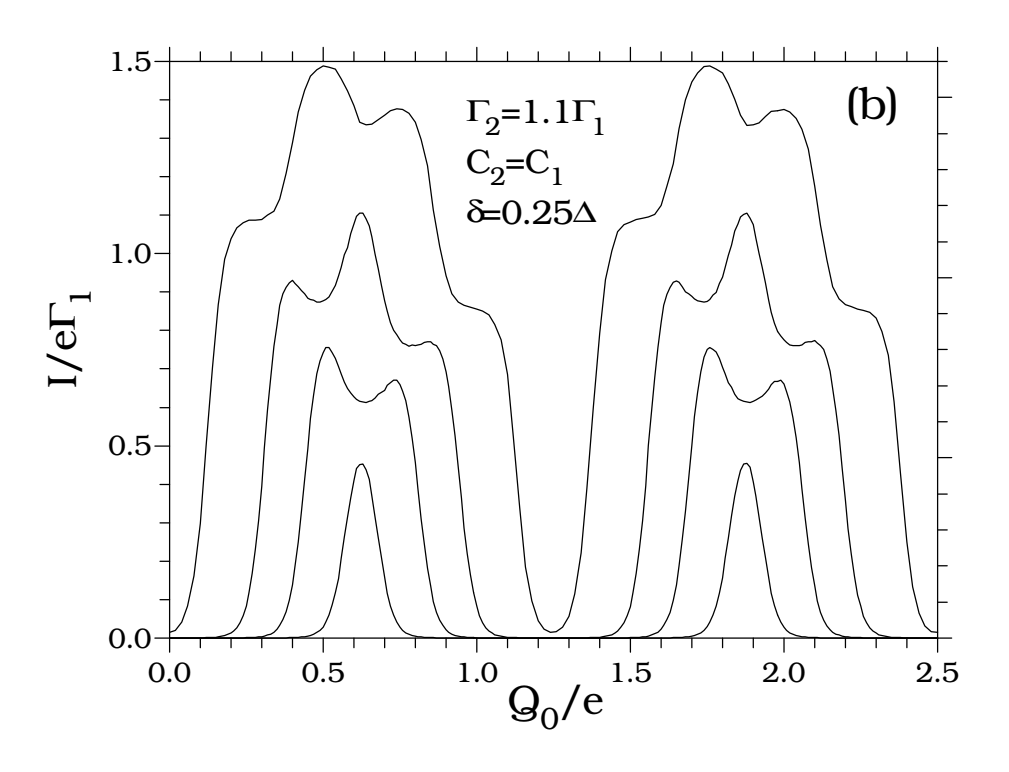
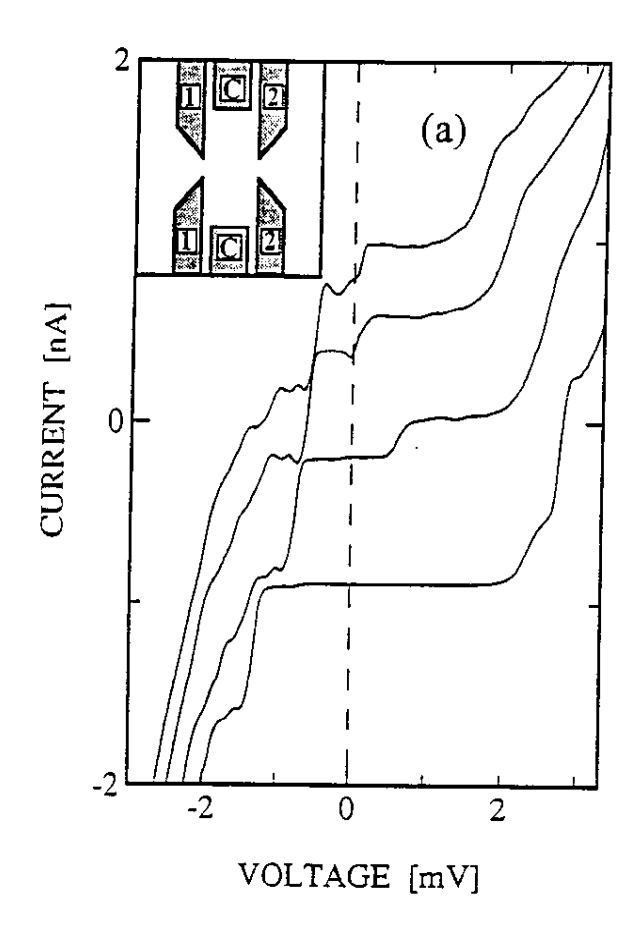


Fig. 14



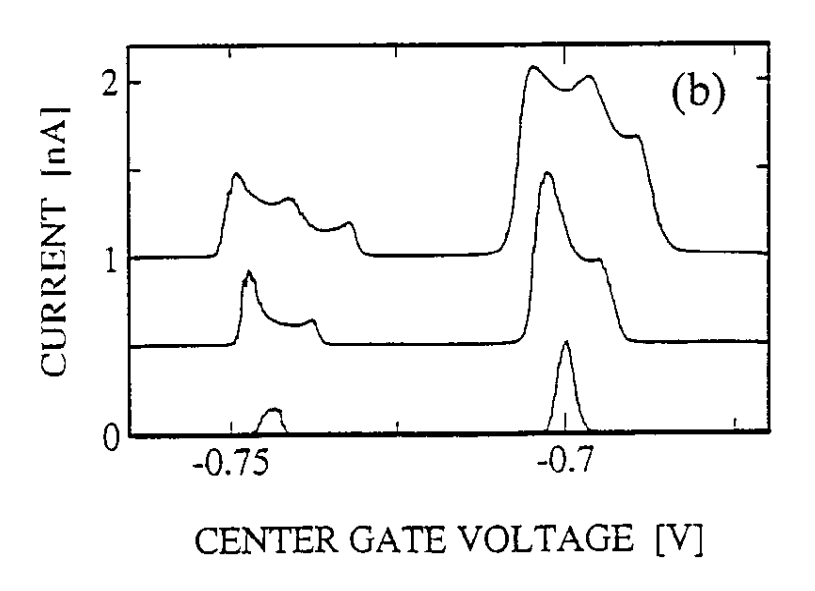


Fig. 15